ADVANCED PHOTONICS RESEARCH
Open Access
www.adpr-journal.com

Advanced Optical Imaging Technologies for Microplastics Identification: Progress and Challenges

*Yanmin Zhu, Yuxing Li, Jianqing Huang, Yunping Zhang, Yuen-Wa Ho, James Kar-Hei Fang, and Edmund Y. Lam**

Global concern about microplastic (MP) and nanoplastic (NP) particles is continuously rising with their proliferation worldwide. Effective identification methods for MP and NP pollution monitoring are highly needed, but due to different requirements and technical challenges, much of the work is still in progress. Herein, the advanced optical imaging systems that are successfully applied or have the potential for MP identification are focused on. Compared with chemical and thermal analyses, optical methods have the unique advantages of being nondestructive and noncontact and allow fast detection without complex sample preprocessing. Furthermore, they are capable of revealing the morphology, anisotropy, and material characteristics of MP for their quick and robust detection. This review aims to present a comprehensive discussion of the relevant optical imaging systems, emphasizing their operating principles, strengths, and drawbacks. Multiple comparisons and analyses among these technologies are conducted in order to provide practical guidelines for researchers. In addition, the combination of optical and other alternative technologies is described and the representative portable MP detection devices are highlighted. Together, they shed light on the prospects for long-term MP pollution monitoring and environmental protection.

The name microplastic (MP) was coined by Thompson et al.[1] in Science in 2004, referring to plastic particles of size 1 μm–5 mm. According to their sources, they are further categorized into primary and secondary MPs.[2] Primary MPs come from manufactured plastic microfibers and microparticles, which are usually found in textiles, medicines, and personal care products. For example, microbeads[3] used for facial cleanser and toothpaste are dispersed in wastewater and eventually enter the aquatic environment, contributing to the pollution of MPs in water.[4] Secondary MPs originate from large-scale plastic materials that break down through natural weathering, mechanical abrasion, biological reaction, or human activities.[5] The degradation of plastics is location dependent and influenced by various factors, such as solar radiation, water, temperature, and oxygen content. Tire wear particles[6] and synthetic plastic fibers released from the laundry processes[7] are two representative examples of secondary MPs. When the size of MPs is further reduced below 1 μm, they become nanoplastics (NPs), increasing the difficulty substantially in combating plastic pollution.[8]

Over the past decade, many researchers have considered the proliferation of MPs in air, soil, and water as among the most serious forms of pollution.[9] An article in Science reported that 4.8–12.7 million tons of plastic waste were deposited from the land into the ocean in 2010.[10] Additionally, as reported by Sebille et al.[11] in 2015, the total number of MP particles on surface waters globally was estimated between 15 and 51 trillion. Although various efforts have been devoted to reducing and recycling plastics in some countries, most plastic litter remains untreated. Due to the increasing

Y. Zhu, Y. Li, J. Huang, Y. Zhang, E. Y. Lam
Department of Electrical and Electronic Engineering
The University of Hong Kong
Hong Kong SAR, China
E-mail: yuxingli@hku.hk; hjq2026@hku.hk; elam@eee.hku.hk

Y. Zhu
Department of Mechanical Engineering
Massachusetts Institute of Technology
Cambridge 02139, MA, USA

The ORCID identification number(s) for the author(s) of this article can be found under https://doi.org/10.1002/adpr.202400038.

DOI: 10.1002/adpr.202400038

J. Huang
Key Lab of Education Ministry for Power Machinery and Engineering
School of Mechanical Engineering
Shanghai Jiao Tong University
Shanghai 200240, China

Y.-W. Ho, J. K. H. Fang
Department of Food Science and Nutrition
The Hong Kong Polytechnic University
Hong Kong SAR, China

J. K. H. Fang
State Key Laboratory of Marine Pollution
City University of Hong Kong
Hong Kong SAR, China

generation of MPs and their resistance to quick decomposition, the actual number of MPs today is certainly much higher. However, it remains challenging to perform accurate MP pollution assessments on a global scale.

MPs have harmful impacts on wildlife, human health, and ecosystems.[12–15] Most MP samples found in natural environments have various materials, including polymethyl methacrylate (PMMA), polyethylene (PE), polyethylene terephthalate (PET), polycarbonate (PC), polypropylene (PP), polystyrene (PS), and polyvinyl chloride (PVC). Certain additives, such as plasticizers, are added to plastic products to perform specific functions, which often remain within the plastic fragments. In addition, with a large specific surface area and small size, MPs may attach to the toxic substances, such as heavy metal elements, bacteria, and viruses.[16,17] Worse, along the food chain, MPs are often ingested by organisms and adhere to the surface of cells. These harmful substances continuously affect the cells' activities and even cause abnormal mutation or apoptosis.[18] For example, researchers found that PVC MPs can induce cytoplasmic vacuolation in the liver, glomeruli tuft shrinkage, and aggregation of melanin macrophage cells in the kidney.[19] Unfortunately, as humans are at the top of the food chain, MPs are high-likely to accumulate in the human body. The adverse effects of MPs on human health include, but are not limited to, headache dizziness, liver dysfunction, respiratory failure, and eye vision failure.[20] Besides, researchers also found that MPs have a remarkable negative influence on the soil ecosystem, reducing bacterial diversity while increasing fungal diversity and enzyme activity.[21] **Figure 1** illustrates the source and migration of MPs in real environments. The circular arrows indicate the migration of MPs in air, soil, water, and accumulation in the human body.

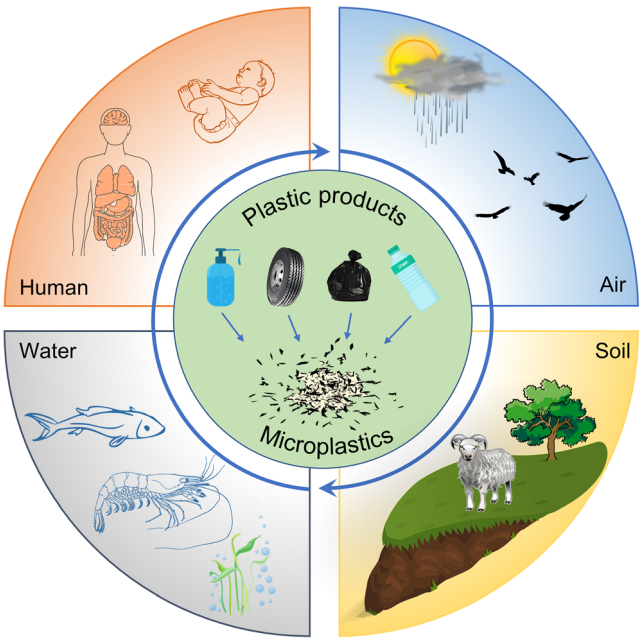

Figure 1. The source and migration of MPs. Originating from plastic products, MP particles disperse in air, soil, and water and migrate along the food chain. Eventually, the accumulation of MPs has harmful effects on human health.

Consequently, with increasing scientific interests and public health concerns, it is imperative to develop efficacious detection methods for MP pollution assessment.[22,23] Accurate acquisition of physicochemical properties is the basis for understanding the origin, pathway, and impact of MPs, thereby establishing MPs suppression or removal strategies.

Conventionally, one would sample the soil or water and bring the samples to the laboratory for MP separation and detection. Chemical and thermal analyses of the MPs are the most commonly adopted methods in the laboratory. The former, such as Fourier-transform infrared spectroscopy (FTIR),[24] Raman spectroscopy,[25] and optical photothermal infrared spectroscopy,[26] can distinguish different types of MPs from the captured infrared spectra of the samples. The latter, such as pyrolysis–gas chromatography–mass (pyrolysis–GC–MS) spectrometry[27] and thermal extraction desorption–GC–MS (TED–GC–MS),[28] is capable of identifying the polymer types and quantities through analyzing the characteristic pyrolysis spectra of the sample. However, these methods often require labor-intensive and time-consuming pretreatments of the samples, such as the MP sampling approaches and preparation methods reviewed by Stock et al.[29] Furthermore, these methods need further improvement when it comes to the slow scanning speed (typically dozens of seconds for one testing spot using FTIR), which results in a low-analysis throughput. Finally, the equipment for chemical and thermal analyses of MPs is rather expensive, limiting their availability in laboratories. Thus, there is a strong need to simplify the detection procedures and improve measurement efficiency for MP pollution assessment.

More recently, imaging-based methods are increasingly demonstrating their power and advantages in MP detection and analysis. Holographic imaging, hyperspectral imaging, and polarization imaging are typical examples that have been successfully used for MP identification and characterization. They are capable of obtaining various information from the MP images, including morphological, optical, and chemical features. For instance, thickness, surface roughness, refractive index, and birefringence of plastic materials can be determined simultaneously with its spectral response.[30,31] The distinctive advantages of these imaging-based MP detection methods are their relatively simple optical setup and fewer sample preparation procedures, making them ideally suitable as field-portable systems that can realize in situ environmental monitoring, and perform a high-throughput analysis of MPs in various scenarios. Despite these advantages, more efforts need to be made, due to the variations in MP properties (e.g., material, shape, size, hydrophobicity, aging, etc.) and measurement conditions (e.g., temperature, pressure, water, illumination, etc.) to improve the robustness of these methods.

The main motivation for this review is to summarize and discuss recent advances in imaging-based methods that have been reported for the detection, identification, and characterization of MPs. We classify them into two main categories, according to their application scenarios: microscopy employed in the laboratory environment and optical imaging technologies for in situ detection. The former relies on sophisticated microscopy equipment and can offer a high spatial resolution. The latter is relatively simple, lightweight, and portable and usually has a high degree of integrated automation. For both, we introduce and

compare the principles, typical applications, advantages, and limitations of these methods. Furthermore, building a portable high-throughput MP monitoring system is a highly desirable goal, and here we present the main challenges, current solutions, and future research directions in this area. In particular, we will highlight the potential of holographic imaging for MP identification and analysis.

1. Microscopy Employed in the Laboratory Environment

Microscopic techniques are the most commonly utilized methods for the physical characterization of MPs, as they provide detailed structural information for identification purposes.[32] A range of microscopic techniques, notably stereomicroscopy, fluorescence microscopy, scanning electron microscopy (SEM), transmission electron microscopy (TEM), and atomic force microscopy (AFM), are widely employed in laboratory settings. Each of these techniques has unique imaging capabilities and is suited for particular applications.

However, a single imaging method often proves insufficient to accurately and reliably identify MPs, which may vary widely in size, shape, and polymer composition, particularly when they are embedded in complex environmental matrices.[33] As a result, the combination of two or more analytical techniques is often used to overcome these limitations. Typically, physical characterization is coupled with chemical characterization, such as spectroscopy, to produce a comprehensive analysis.

In this section, we present an overview of the five representative optical imaging techniques for MP detection in the laboratory, covering their principles, characteristics, sample preparation, and typical applications. Additionally, we illustrate the integration of each microscopy technique with spectroscopy through specific examples. To conclude the section, we provide a comparison and discussion of these microscopic techniques, offering an intuitive understanding and serving as a guide for selecting the most appropriate method.

1.1. Stereomicroscopy

The stereomicroscope is a conventional microscope that is designed for low-magnification observation of samples. It can produce an upright, 3D image based on reflected light from the objective surface. The working principle of a stereomicroscope is to observe the samples by two separate optical paths of slightly different angles, which produces stereoscopic vision.[34]

The stereomicroscope has a comprehensive imaging capability with a long working distance, which makes it easy to operate and widely applicable in various fields such as biological observations[35] and engineering sedimentation measurement.[36] However, the relatively low magnification power of stereomicroscope, typically between 6 and 100 times,[37] limits the observations of samples that are less than 50 μm.[38]

In the context of environmental studies, stereomicroscopes are extensively applied for the observation and identification of MPs larger than a few hundred micrometers based on their physical appearance. Prior to observation, MPs need to be separated and filtered to facilitate more precise imaging. Furthermore, information on MP surface structure, such as color, size, and shape, is recorded and categorized, which is significant for a better understanding of MP particle typology.[39,40] For further characterization, imaging software such as ImageJ is widely used to analyze data extracted from the sample images.[41] However, it is challenging to characterize particles smaller than 100 μm, particularly when they are transparent or have unusual shapes.[42]

While the stereomicroscope is an effective and convenient way to observe MPs based on physical characteristics, it is inherently subjective as it relies heavily on visual identification by the observers. Therefore, the subjectivity can potentially result in the over- or underestimation of MP abundance. In addition, limitations in sample preparation and size observation may further impact the accuracy of detection results, which can account for 20–70% of all MPs as per subsequent characterization by other techniques.[43] The identification of synthetic and natural fibers, which are abundant in water, sediment, and biota samples, presents additional challenges when using a stereomicroscope.

To obtain more accurate detection results, a stereomicroscope can be used in combination with other detection methods, such as spectroscopy.[39] For instance, the combination of a stereomicroscope and FTIR identification methods has been employed for detecting samples from the sea surface microlayer and beach sand.[42,44] Choosing suitable characterization techniques is essential for accurately evaluating the extent of MP pollution.

1.2. Fluorescence Microscopy

A fluorescence microscope is an optical microscope that uses short-wavelength light to excite a measured substance to emit fluorescence, allowing for the observation and localization of fluorophores in samples for qualitative and quantitative research.[45,46] Fluorophores may be naturally present in the samples or introduced via fluorescent dyes for substances that lack inherent fluorescence.

Fluorescence microscopy has the advantage of high specificity and sensitivity, and enables the detection of trace amounts of substances even at low fluorescent dye concentrations, making it a popular choice in the studies of biological specimens involving cells and bacteria. Additionally, fluorescence microscopy has demonstrated its effectiveness in the identification of MPs in various laboratory studies.[47,48] Excitation wavelengths commonly used for MP detection include 390 nm (blue fluorescent), 542 nm (red fluorescent), and 475 nm (green fluorescent).[49]

Fluorescence microscopy can have a simple setup, such as with an epifluorescence microscope,[50,51] or more complex configurations, such as confocal optical and two-photon microscopy. Confocal optical microscopy has certain specific tomographic capabilities, which use optical sectioning to obtain a high-resolution fluorescence image.[52] It has been able to image the uptake of PS plastic beads of different sizes (ranging from submicrometer to micrometer size) by plant tissues.[53] In comparison, two-photon microscopy is based on multiphoton absorption, providing an increased penetration depth of samples, higher light detection efficiency, and reduced photobleaching. Therefore, it is a superior alternative to confocal microscopy

when distinguishing samples with autofluorescence, such as algae, from MPs.[54]

Fluorescence microscopy has been used to detect and quantify white and transparent plastics based on their innate ability to emit fluorescence,[55] an alternative to stereomicroscopy, which has difficulty detecting transparent MPs. Furthermore, combined with Nile Red dye staining, fluorescence microscopy expands the variety of detection, such as MPs in bottled water[56] and even in remote places with limited access to expensive resources.[57] The range of measurable substances can continue to expand with the invention of new fluorescent dyes.

While fluorescence microscopy is a sensitive and quantitative tool for MP observation and identification, it also has limitations that can lead to miscalculations. For instance, plastic materials typically exhibit significant fluorescence or autofluorescence when exposed to near-UV or visible light. However, the presence of organic matter on filters may prevent the identification of polymeric particles because of the costaining of biological material and impeding of polymeric particle reflection.[58] Additionally, chemical additives in plastic compositions may also show fluorescent features and interfere with quantifying fluorescence characteristics.[59]

Overall, fluorescence microscopy is a relatively cost-effective and quick method for MP detection, but it should be used in conjunction with other methods to avoid potential inaccuracies.

1.3. Scanning Electron Microscopy

SEM is a powerful observational technique that utilizes a narrow, focused, high-energy-electron beam to examine the sample and stimulate physical information through the interaction between the beam and the substance. The collected images are then amplified and reconstructed to characterize the microscopic morphology of the substance. It is a multifunctional technique with many superior properties, including high resolution, which can reach 1 nm,[60] and magnification that can be continuously adjusted to achieve 300 000 times or more. Additionally, SEM enables the realization of 3D shape observation and analysis and is widely used in the research of various materials, including rock and soil, graphite, ceramics, and nanomaterials.[61] Furthermore, integrating SEM with other analytical instruments allows for the observation of microscopic morphology and analysis of the microregion composition of the material, enhancing SEM's utility and broadening its application scope.[62]

To prepare for SEM analysis, there is no requirement for a particular digestion method to eliminate the organic matter from samples. However, before the microscopic examination, pretreatment is necessary, involving the coating of sample targets with a conductive layer of metals such as platinum, gold, or carbon.[63]

The high resolution of SEM makes it an ideal method for identifying the detailed surface morphology of MPs. SEM has been applied to detect atmospheric MP morphology and monitor the corresponding degradation.[64,65] Furthermore, while observing the morphology, SEM can conduct component analysis for the MP microarea. For example, MP particles were analyzed using SEM to identify their content of inorganic plastic additives.[66]

The methodology of SEM has been widely utilized in examining MPs obtained from different sources within the aquatic ecosystem, particularly from various types of water samples such as seawater, river water, lake water, and wastewater.[67] Also, SEM analyses predominantly center on characterizing the morphological features of small-scale MPs. However, SEM has corresponding limitations when it comes to detecting numerous samples, which result from its limited maneuverability, high cost, and low detection numbers.[65]

In short, SEM is a powerful tool for scientific research with a wide range of applications in various fields, including MP analysis. However, the limitations of SEM must also be considered when conducting research, particularly when analyzing numerous samples.

1.4. Transmission Electron Microscopy

TEM is a widely employed strategy for analyzing nanomaterials in electron microscopy. It provides the chemical composition and physical shape of nanomaterials with an atomic-scale spatial resolution. TEM can observe the submicrometer structure or ultrastructure that cannot be seen clearly under the optical microscope, and its resolution can reach 0.2 nm.[68] Choosing a light source with a shorter wavelength is necessary to improve the resolution and detect surface structures.

The working principle of TEM is to project an accelerated and concentrated electron beam onto an ultrathin sample. The wavelength of the electron beam, 2.pm at 200 keV, is much shorter than that of visible light and ultraviolet light, which allows electron microscopes to produce higher-resolution images. The electrons collide with the atoms in the specimen and change their direction, thus creating a solid angle scattering. The scattering angles vary according to the density and thickness of the sample, so the image is formed accordingly with different levels of brightness. After zooming in and focusing, the images are further displayed on imaging devices, such as fluorescent screens, films, and photosensitive coupling components.

Due to its high resolution and sensitivity, TEM can detect slight deformation of MPs. TEM can examine the dislocation state between the surface and interior of a material under various stress conditions.[69] Also, the existence of plastics within soil fractions has been studied using morphological and analytical characterization by TEM linked with energy-dispersive X-ray spectroscopy (TEM–EDX) and pyrolysis–GC–MS.[70]

Because TEM can only examine very thin samples, the sample preparation step is more labor intensive and time consuming, since the structure of the material surface may be different from the inner structure of the material. Meanwhile, the preparation process of the ultrathin sample (less than 100 nm) is complicated, and the samples are prone to damage during this procedure. The application of TEM is limited to the detection of MPs and NPs. So far, no NPs have actually been detected in soft matrices by TEM, and the main reason is that the amorphous character of NPs restricts TEM visualization efficiency. Besides, additional heavy metal stains are required for the polymer elementary composition analysis, as the organic elements of polymers have a weak contrast in the TEM imaging process based on the ineffective elastic interaction of these components with an electron beam.[37]

1.5. Atomic Force Microscopy

The AFM is a sophisticated tool designed to analyze the surface composition of various solid materials, including insulators, with a resolution surpassing the optical diffraction limit by over 1000 times, reaching down to only a fraction of a nanometer.[71] The AFM can determine the surface properties and structures of different materials by examining the incredibly subtle interatomic interaction between the test sample's surface and a miniature force-sensitive component. A pair of microcantilevers, sensitive to faint force, is employed in this process, with one end secured and the other end's tiny tip positioned near the sample. Both ends interact with each other, and the force results in deformation or alterations in the microcantilever's motion. AFM uses a sensor to assess these changes while scanning the sample, which subsequently reveals information about the surface topography structure and roughness at a nanometer scale.[72,73]

AFM offers several benefits compared to SEM. First, AFM provides actual 3D maps of surfaces, whereas electron microscopes only produce 2D pictures. Second, AFM eliminates the need for specific sample treatments, such as copper plating or carbon plating, thus preventing potentially irreversible harm to the specimen. Third, while electron microscopes require high-vacuum conditions to function, AFMs can operate effectively under standard pressure or even in liquid settings, so the preparation of samples is more convenient and applicable.[74,75]

Therefore, AFM has been widely used for the characterization of a variety of nanoscale samples in scientific research and industry, including soil particles,[76] engineered nanoparticles, polymeric membranes,[77] and other nanostructures.[78] AFM has been used to visualize the uptake and distribution of PS particles in human skin fibroblasts. Particles as small as 500 nm were captured in fully fixed cells, and the nanomechanical characterization facilitated distinguishing between the internalized and surface-adhered plastics.[79] Moreover, AFM allows for identifying materials in polymer mixtures and determining compounds adsorbed onto the MP surface.[80] Additionally, AFM can be combined with other detection technologies, such as infrared-related techniques, to investigate the nanoscale infrared, thermal, and mechanical characteristics of aging MPs.[81]

In summary, AFM can provide additional parameters such as stiffness, hydrophobicity, conductivity, or magnetization. However, AFM has some disadvantages, including a limited imaging range, slow speed, extreme sensitivity to the probe, and a high cost.

1.6. Comparison and Discussion

When selecting a detection method for MP identification, there is a trade-off between resolution, portability, ease of operation, and the cost of the equipment. Each detection technique comes with its own advantages and limitations and can be used either independently or in combination with others to detect MPs in various environmental samples. **Table 1** provides a comprehensive comparison of the different imaging methods available for MP detection.

The choice of imaging methods relies on factors such as the specific application, desired resolution, and available resources. Using multiple imaging techniques can complement each other, offering a more complete understanding of MP properties in environmental samples.

In what follows, we present a detailed comparison of the five representative optical imaging techniques, examining them from three specific aspects: resolution and field of view, preprocessing, as well as portability and cost. Our goal is to offer a comprehensive reference for choosing the appropriate imaging tools for MP identification.

1.6.1. Resolution and Field of View

In most imaging systems, there is often a trade-off between resolution and field of view. For MP detection, high-resolution imaging allows for the observation of fine details and structures of the MP surface, but it limits the area that can be observed at a particular time. Conversely, a larger field of view enables the observation of a broader area of the sample, but the resolution may be too low to discern fine details.

Stereomicroscopy provides among the lowest resolution, generally $>50\,\mu m$, but with a large field of view, making it suitable for observing larger MPs and obtaining 3D information.[37,38] In contrast, fluorescence microscopy offers a higher resolution, typically down to ≈ 200 nm, allowing for more detailed visualization of smaller particles. However, the field of view in fluorescence microscopy is generally smaller compared to stereomicroscopy, which may limit its applicability for large-scale or whole-sample observations. Nevertheless, fluorescence microscopy is particularly useful for detecting fluorescent or labeled particles in complex samples.[55]

SEM and TEM are electron microscopy techniques that offer significantly higher resolution than optical techniques. SEM has a resolution ranging from 1 to 10 nm and a smaller field of view than optical techniques, making it ideal for studying surface morphology.[60] TEM provides even higher resolution at the subnanometer scale but has a more limited field of view.[68]

AFM offers ultrahigh-resolution imaging (subnanometer to several nanometers) and a smaller field of view than SEM and TEM. It provides 3D information about the surface topography of MPs and can operate in an air or liquid environment.[71] However, AFM has a slower imaging speed and requires the sample to be immobilized on a flat, rigid surface.

To summarize, stereo and fluorescence microscopy are more suitable for the counting and rough size measurement of larger MPs, with fluorescence microscopy being particularly useful for detecting fluorescent or labeled particles. SEM and TEM provide high-resolution images but require sample preparation and vacuum conditions, while AFM offers high-resolution, 3D imaging in air or liquid environments but with a smaller field of view and slower imaging speed. The representative images are presented in **Figure 2** and the choice of microscopy technique depends on factors such as particle size, required resolution, sample preparation, and environmental conditions.

1.6.2. Preprocessing

When comparing the ease of operation and preprocessing requirements for MP identification and quantification among various microscopy techniques, it is evident that stereo and

Table 1. Comparison among several microscopic methods in the laboratory.

Method[a)]	Stereomicroscopy	Fluorescence microscopy	SEM	Transmission electron microscopy	Atomic force microscopy
Resolution	Generally limited detection to $>50\,\mu m$	From 180 nm in the focal plane and to about 500 nm along the optic axis	2 nm at 2 Kv	0.2 nm	Vertical distance resolution of better than 0.1 nm
Advantage	–Simple –Fast –Low cost –Easy to operate	–Easy –Detection of transparent particles –Immediate visualization of the particles	–Clear and high-resolution images of particles –Elemental analysis of particles if coupled with EDS. –No gas into the chamber if coupled in ESEM mode. –Small detected particles in STEM mode. –No treatment of sample in FESEM mode	–Very high resolution (<0.1 nm). –Elemental analysis of particles if coupled with EDS. –Analytical capabilities with EELS.	–No radiation damage of the sample. –Preserved sample surface. –3D images of the surface structure of the polymers. –Best resolution obtained (0.3 nm).
Limitation	–No chemical conformation. High possibility of false positive. –High possibility of missing small and transparent plastic particles. –Greatly influenced by researchers' knowledge.	–Laser in the ultraviolet can be harmful and toxic for the sample. –Chemical additives can interfere with fluorescence.	–Expensive, –Time-consuming. –Lack of information on the type of polymer. –Colors cannot be detected.	–Very expensive. –Ultrathin sample (less than 100 nm) required.	–No prevention from outside factors such as contaminations. –Damage caused by the interaction of the tip with the sample.
Typical applications	–To obtain the size, shapes, colors, numbers. –To enumerate suspected MPs.	–To identify transparent MPs based on their innate ability to emit fluorescence	–To obtain the morphology of MPs. –By combining it with EDS, the MP elements can be detected.	–To characterize nanomaterials. –To detect slight deformation of MP.	–To provide true 3D maps of surfaces. –To characterize a variety of nanoscale samples.
Setup					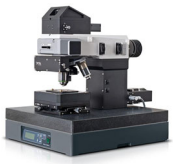
References	[38,42]	[45,47]	[62,202]	[69,78]	[71,72,203]

[a)]EDS: energy-dispersive spectrometer, ESEM: environmental SEM, STEM: scanning TEM, FESEM: field-emission SEM, EELS: electron energy loss spectroscopy.

fluorescence microscopy are easier to operate and require less preprocessing compared to SEM, TEM, and AFM.

Stereomicroscopy is relatively simple to operate with minimal sample preparation as shown in **Figure 3**, whereas fluorescence microscopy may necessitate an additional labeling step, such as staining with fluorescent dyes like Nile Red.[56] Despite the extra step, both stereo and fluorescence microscopy remain more straightforward than other advanced techniques.

In contrast, SEM and TEM are more complex to operate and demand specialized training and extensive sample preparation, such as dehydration, coating with conductive material (for SEM),[82,83] or embedding, and sectioning (for TEM).[84] Additionally, both techniques demand high-vacuum conditions to function properly.[85] The required sample preparation and vacuum conditions may alter the properties of the samples, posing a challenge for accurate analysis.

AFM presents challenges in operation due to its sensitive probe–sample interactions and requires sample fixation. Also, calibration and optimization of parameters are also more involved in AFM than other techniques.[86]

In short, stereo and fluorescence microscopy are easier to operate and involve less preprocessing for MP identification, while SEM, TEM, and AFM require more specialized training, complex operation, and extensive sample preparation.

1.6.3. Portability and Cost

Portability and cost are important considerations when selecting appropriate imaging methods. Stereo and fluorescence microscopes are more compact and lightweight, making them suitable for laboratory use. They are also less expensive, with prices ranging from a few hundred to several thousand U.S. dollars,

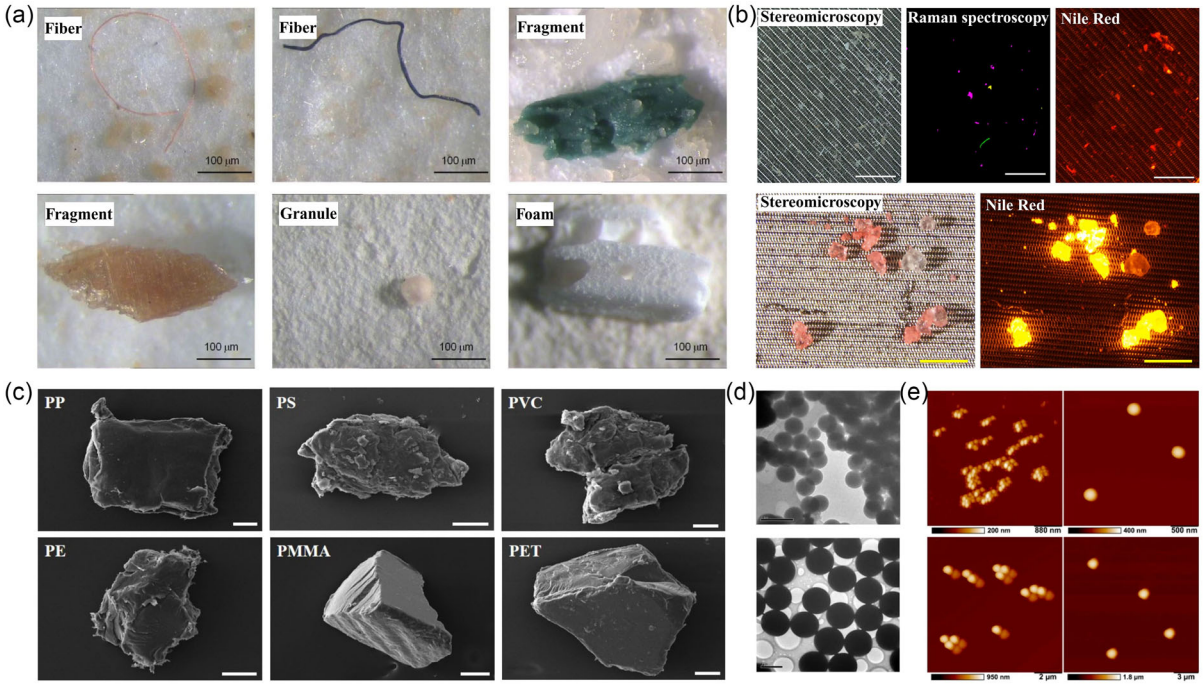

Figure 2. Representative MP images from different microscopy technologies and corresponding resolution demonstration. a) Stereomicroscopic images of MPs found in collected mussels. Scale bar: 100 μm. Adapted under the terms of the CC-BY Creative Commons Attribution 4.0 International license.[199] Copyright 2022, Multidisciplinary Digital Publishing Institute (MDPI). b) MP particles were processed from cryogenic milling and stained with Nile red viewing under the stereomicroscope and fluorescence microscope. White scale bar: 2000 μm and yellow scale bar: 800 μm. c) The SEM images demonstrated different kinds of MPs and corresponding morphological features. Scale bar: 100 μm. Adapted with permission.[25] Copyright 2021, Elsevier. d) The TEM images revealed the primary size and morphology of PS particles in the culture solution. Upper scale bar: 1 μm, and bottom scale: 5 μm. Adapted under the terms of the CC-BY Creative Commons Attribution 4.0 International license.[200] Copyright 2021, Frontiers. e) AFM images of 100 nm, 200 nm, 500 nm, 1 μm PS particles. Scale bar: 880 nm, 500 nm, 2 μm, and 3 μm. Adapted under the terms of the CC-BY Creative Commons Attribution 4.0 International license.[80] Copyright 2022, Multidisciplinary Digital Publishing Institute (MDPI).

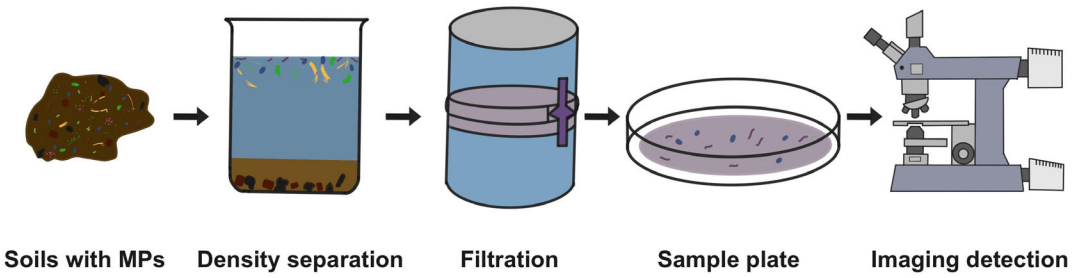

Figure 3. The process of MP sampling for imaging and detection. The soils with MPs are obtained and separated according to varied densities. The plastic samples are further filtrated based on size and isolated from the organic matter. Then, the samples are identified under the corresponding microscopes.

depending on the features and quality. Stereomicroscopes can be used for quick identification of larger MP, while fluorescence microscopes can detect labeled or inherently fluorescent MP particles in complex samples. The cost of fluorescent dyes should also be considered for fluorescence microscopy.

In comparison, SEM, TEM, and AFM are more sophisticated and require a dedicated laboratory environment due to their size, weight, and operational requirements. SEM and TEM require high-vacuum conditions, rendering them less adaptable to portable applications, while AFM requires a stable, vibration-free environment for optimal operation. The cost of these advanced microscopy techniques is significantly higher, with prices ranging from tens to hundreds of thousands of U.S. dollars, depending on the instrument's capabilities and accessories. Additionally, the costs associated with sample preparation, maintenance, and operation of SEM, TEM, and AFM should also be considered.

2. Optical Imaging Technologies for In Situ Detection

Optical imaging technologies provide nondestructive and noninvasive analysis of samples without sample damage or altering or damaging them. They are important for accurate measurements of MP abundance, size distribution, and composition. For example, hyperspectral imaging captures multiple images of the samples at different wavelengths, which provide a spectral signature for each pixel in the image for MP identification.[87] Likewise, polarization imaging has the capability to acquire multiple images of samples exhibiting distinct polarization states. This facilitates the extraction of additional physical details regarding the shape and orientation of the MPs, imparting sensitivity to factors such as the particle's shape, size, and refractive index.[58] Meanwhile, digital holography captures the interference patterns of MPs with rich physical and structural information.[88] It is a powerful imaging technology, without requiring sample preparation or staining, and offers a superior noninvasive real-time in situ detection solution.[89]

In this section, we summarize the working principle and the application situations for hyperspectral imaging, polarization imaging, and digital holography, which are the three main optical imaging technologies used for in situ MPs detection. We also compare spectroscopic and imaging technologies for in situ usage. The advantages and drawbacks of each technology are presented to guide practitioners in using and evaluating various options.

2.1. Hyperspectral Imaging

Hyperspectral imaging can provide a high spectral resolution with a wide range of wavelengths. It is of great importance for MP identification, especially under harsh environmental conditions.[30]

2.1.1. Principle

Hyperspectral imaging is an optical spectroscopy technique that combines spatial and hyperspectral information.[90] It collects the spectral data at each pixel by scanning the specimen in the *x*- and *y*-axis, while acquiring the spectral response along the axial dimension over a number of wavelengths (usually ≈100). As an example shown in **Figure 4**, the system consists of a light source, a digitally controlled sample housing stage, and a hyperspectral camera.[91] Enabled by advanced algorithms,[92,93] it has become a label-free and nondestructive imaging method with high throughput, making it a versatile technique for imaging and quantitative detection of micro- and nanoscale particles from single-shot measurements.

2.1.2. Application of Hyperspectral Imaging in MPs

The MP identification and classification by hyperspectral imaging is based on retrieving polymer composition information of the samples.[94] The generated 3D hyperspectral data (hypercubes) of the targeted objects are collected and analyzed by matching with their reference spectral signatures.[91,95–97] Since hyperspectral imaging generates a massive amount of data (both image and spectral data simultaneously) with much redundant information, it requires further processing techniques, such as data mining, dimensional reduction, and classification algorithms, to obtain useful information. Principal component analysis (PCA) is a common technique to reduce the data dimension, thus avoiding the performance degradation resulting from data redundancy.[91,95,98–100] Serrant et al.[95] acquired hyperspectral images in the short-wave infrared (SWIR) range (1000–2500 nm) to classify floating plastic debris from afar. They used the SWIR camera with 256 wavelengths to collect the hyperspectral images and processed them by PCA to reduce the data dimension. Then, a classifier based on partial least squares discriminant analysis (PLS-DA) is applied on the reference polymer spectra to classify the unknown MP fragments. Alternatively, Zhao et al.[98] used a support vector machine (SVM) as another classifier for detecting household polymers with different colors and sizes (0.5–5 mm) on the soil surface. Gong et al.[101] also demonstrated a similar application of combining machine learning and hyperspectral image technology for the detection of MPs in packaged rice, specifically in the near-infrared spectral region. Its functionality in classifying three of the most commonly occurring MPs (i.e., PP, PE, and PS) is also demonstrated in several following studies.[91,100]

Hyperspectral imaging provides relief for the extensive sample preparation time without the need for pretreatment and

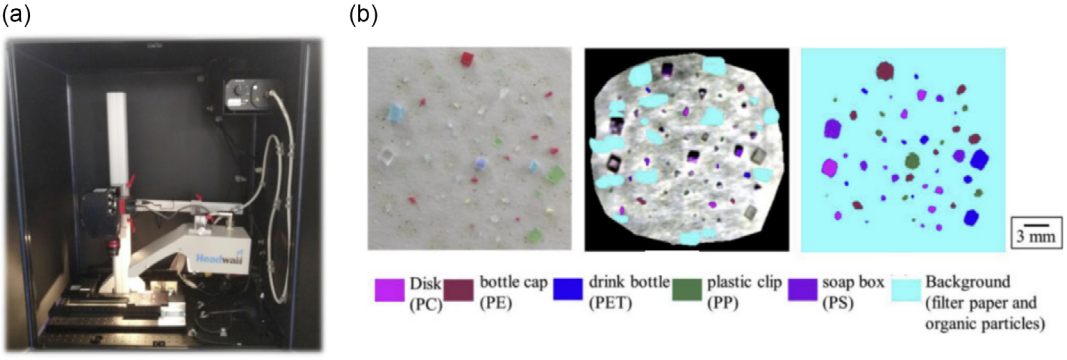

Figure 4. Illustration of (a) hyperspectral imaging system and (b) classification results of common household MP. Reproduced with permission.[91] Copyright 2023, Elsevier.

purification of samples. Without the tedious and time-consuming sample preparation process, it is a faster alternative to traditional polymer analysis methods. Instead of dealing with an individual object, an investigation of a scene containing a number of MPs can be carried out, which makes it appropriate for uniform investigation and online field monitoring.[94] For instance, Zhang et al.[100] discovered five types of MPs (>0.2 mm) with high detection precision (>96%) on different types of fishes (MP-contaminated intestinal tract samples) using hyperspectral imaging with the total investigation time, including both data acquisition and analysis, around 6 min. Additionally, hyperspectral imaging is suitable for researchers with limited resources, as hyperspectral imaging benchtop system can cost only one-fifth of the gold standard in MP assessment using Raman and FTIR spectroscopy.[30]

Nevertheless, hyperspectral imaging also has its own challenges. As with other imaging modalities, the traditional limitations for detection, such as spatial resolution, signal-to-noise ratio, and field of view, affect the smallest detectable particle sizes. To date, we can achieve a robust performance of MP classification accuracy by hyperspectral imaging for particle size within the range of 1–5 mm.[98] The lower limit can be further improved to 0.2 mm by combining with more powerful classifiers.[91,100] Moreover, some of the above limitations are imposed by the hardware parameters. Therefore, potential improvement is suggested by hardware modifications. For instance, using the CytoViva dark-field hyperspectral imaging microscope, which has the highest spatial resolution of all instruments used (0.128 μm),[102] we can potentially achieve an improved limit of detection at 1 μm, making it competitive with the current performance of Raman spectroscopy.[30,103]

Another issue with hyperspectral imaging is the requirement for a custom-built spectral library for different MP classes. A known spectrum is typically needed to classify MPs into distinct categories or polymer types. However, the plastic fragments can undergo degradation subject to environmental reactions, which manifest as large differences in their respective spectrum compared to the reference.[99] Moreover, most naturally occurring MPs exhibit various geometries compared with the standard samples, which are commonly regular shaped (e.g., spherical and uniform sized).[91,99,100] This causes potential light scattering, resulting in deviations in hyperspectral features even with the same type of particles. Therefore, the classification models built on the standard reference need to consider such alterations in the spectra signatures. From this perspective, a more solid understanding of the degradation effects, as well as the size and geometry effects, on the hyperspectral data of the polymers can contribute to a more robust environmental plastic discrimination and identification. In addition, the reference library can include the field samples, whose polymer type is confirmed by FTIR in advance.[104] After training of the learning algorithms, the model can be generalized to identify MPs from the test samples taken from similar habitats.

In summary, hyperspectral imaging can obtain information on the abundance, size, shape, and polymer type for the whole ensemble of plastic particles in each sample from a single hyperspectral image, reflecting its potential in MP detection under laboratory and field conditions. However, the research on the aforementioned challenges is still in its early stages. Currently, some practitioners add hyperspectral imaging as a preliminary investigation step to replace the visual inspection, followed by verification via FTIR/Raman on the stand-out samples to achieve a more accurate representation of MPs in the targeted sample.[94]

2.2. Polarization Imaging

Polarization imaging analyzes the polarized ellipticity angle and the major optical axis and can distinguish different MPs based on their unique optical and structural properties, such as the degree of crystallinity, birefringence, the presence of additives, etc. Therefore, polarization imaging can potentially estimate the sample's size, shape, and concentration and is useful for the identification of plastic fragments.

2.2.1. Principle

Polarization imaging measures the polarization state of light interacting with a sample. These systems generally have a polarizer–analyzer pair and detect the specimen-induced difference by inspecting the changes in the Jones matrix.[105] The amplitude and the polarization state of the incoming light source are modulated by the specimen and can be used for retrieving its material information.[105]

2.2.2. Application of Polarization Imaging in MPs

Most of the MPs are made of synthetic polymers. Therefore, they can have a high degree of birefringence, with different refractive indices in different directions. Their structural specificity exhibits polarized light behavior, such as reflection, refraction, and scattering, which allows them to be distinct from other types of materials.[106]

A polarization imaging setup for material analysis generally consists of several components, including a light source, polarizers, an electronic detector, and an analyzer, as shown in **Figure 5**. The specific components and configurations of the system vary with the application and the required system sensitivity. A white light or a monochromatic laser is typically selected as the light source to provide system illumination. Polarizers are used to generate and control the polarization state of the light in the system. For instance, a polarization light can be generated with the use of a linear polarizer or a generator. An analyzer is set to detect and analyze the polarization state changes. The analyzer could be both a simple linear polarizer oriented at a specific angle relative to the first polarizer or a more complex one that can

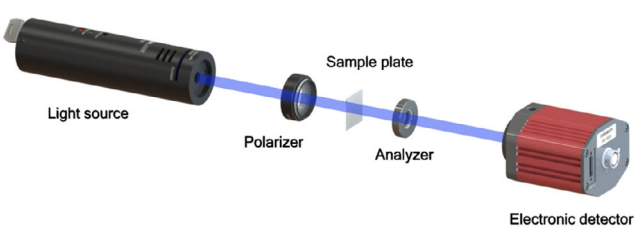

Figure 5. Typical polarization imaging setup for material analysis and sample identification.

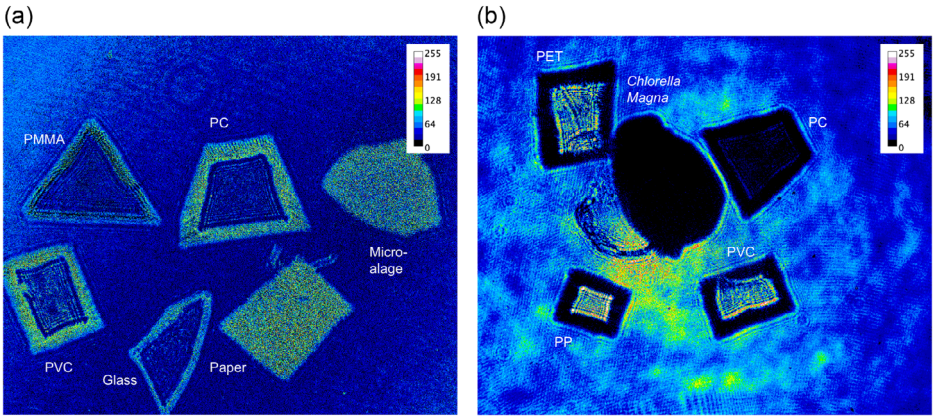

Figure 6. Images from a polarization holographic system.[108] Experimental samples include a) PC, PMMA, PVC, microalgae, paper, and glass. b) PET, PP, PC, PVC, and *Chlorella Magna*.

measure multiple polarization states simultaneously.[107] An electronic detector is normally set as a recorder for image capture. In specific applications, they can also be equipped with additional filters or objectives to improve imaging effectiveness.

The feasibility of using polarization imaging for MP identification, counting, and separation has recently been demonstrated in a multitude of works. Zhu et al.[108,109] developed an intelligent polarization holographic imaging system to record multimodel discriminative image features, such as phase retardation and holographic fringes contrast. Two sets of experimental images are shown in **Figure 6**. MP specimens manifest as different signatures in the images with 1) paper, glass, microalgae and 2) *Chlorella Magna*. This system extracts the physical fingerprint to identify MPs with morphological, textual, polarization, and holographic features. It shows a powerful differentiation capability for material analysis and has the potential for accurate field detection. Meanwhile, Labbe et al.[110] set up a stereomicroscope adaption that can be quickly switched between bright-field, polarization, and fluorescence microscopy modes. Polarization imaging is registered with Nile Red fluorescence imaging for material confirmation. They used such a system to classify MP fibers and natural materials. Sierra et al.[106] also demonstrated the capability of polarization imaging for identifying MPs in the range of $70-600\,\mu m$. They used polarization microscopy to observe the birefringence behavior changes of MP samples with and without mechanical stress and succeeded in identifying anisotropic birefringence material (such as PE, PP, and PET). However, this system is not suitable for nonbirefringence materials such as PVC. Moreover, the reliability of the experimental results is influenced by the sample thickness.

Overall, polarization imaging provides abundant optical and physical information for MP identification. They can then be analyzed by machine learning classification and regression methods, which can result in rapid in situ MP identification. However, one important challenge that needs to be tackled is the detection of opaque particles. In addition, there are several roadblocks to polarization imaging for MP identification. For example, the small plastic fragments are often present in sediment or water, which may change their optical properties. Sample preprocessing, such as filtering or centrifugation, is required to isolate and concentrate the plastic before imaging. In addition, the optical properties of MPs vary with their size, shape, and composition, as well as their ambient environment, which makes it difficult to distinguish them from other materials with similar optical properties. For example, natural fibers or minerals may be misclassified with MPs under polarization imaging. Machine learning or deep learning algorithms could be an efficient solution for identifying MPs in complex samples. Last but not least, polarization imaging requires careful alignment and calibration, which is nontrivial. The image quality may suffer from the unsatisfactory system alignment.

2.3. Digital Holography

Digital holography, as an interferometric imaging technique, encodes wavefront information of the objects into the interference patterns.[111] Holographic interferometry is a technique that quantifies the optical path difference between two coherent beams, providing insights into the object's material. More specifically, holographic interferometry exhibits a high sensitivity toward variations in the refractive index and deformations in the surface morphology of transparent and semitransparent objects. This sensitivity makes it a valuable tool for the identification and analysis of MP. In recent years, digital holography has demonstrated superior detection capabilities for in situ MP detection,[96,112–119] making it a crucial instrument for environmental monitoring and research.

2.3.1. Typical Digital Holography Setups for MP Detection

In a typical digital holography system, the formation of the holographic fringe pattern is achieved by the spatial superposition of the complex reference wave (U_R) and object wave (U_O). U_R and U_O are originally plane waves. A wavefront deformation is introduced in U_O with the reflection, transmission, and scattering from the object. A photodetector (e.g., charge-coupled device and complementary metal-oxide-semiconductor camera) is used to record the intensity distribution ($I(x,y)$) of the resulting holographic patterns.

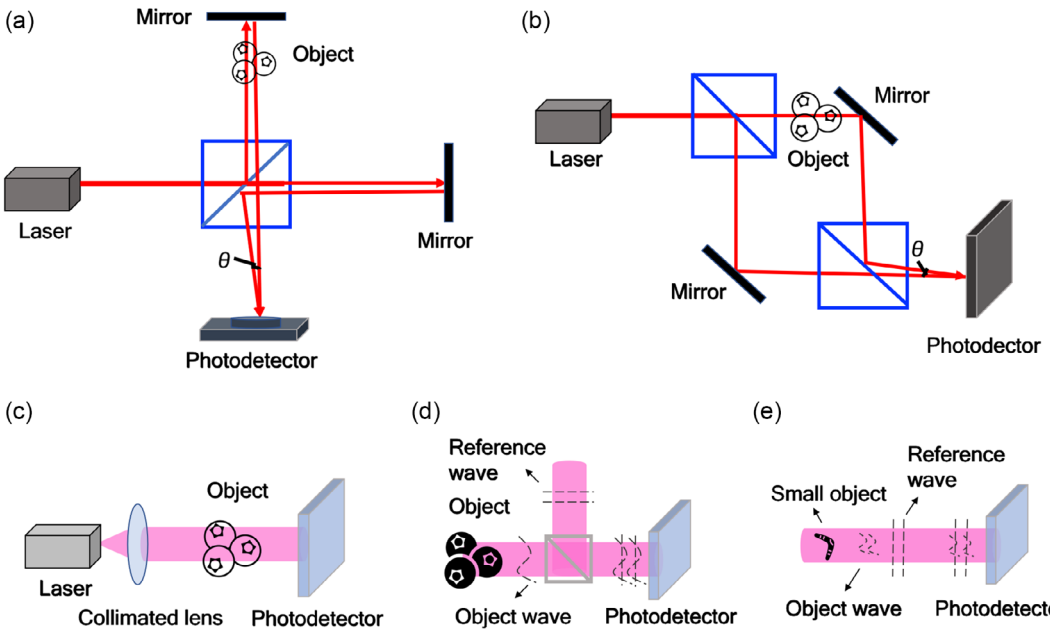

Figure 7. Schematic diagrams of typical digital holographic systems. a) The Michelson interferometer and b) the Mach–Zehnder interferometer. θ is the offset angle between the reference light and the object light; c) a general system structure of in-line digital holography; d) the typical optical path of an in-line digital holography configuration, and e) the in-line Gabor holography configuration. In Gabor holography, the interference appears between the scattered light from the object and the unscattered reference light from the same light beam.

Various interferometric setups are adapted for MP imaging and detection, including off-axis Michelson and Mach–Zehnder interferometry, in-line holography, and Gabor holography.[112,113,116,120,121] Representative setups of these systems are shown in **Figure 7**. In the setup of off-axis digital holography, there is an angle between the reference light and the object light. The twin image and object image are separated by the offset angle, while presumably limiting the system's depth of focus. As shown in Figure 7a,b, the Michelson interferometer records the object information via reflection and the Mach–Zehnder interferometer through transmission. The latter option provides enhanced flexibility in optical design,[122] allowing for feature modulation (such as phase, intensity, and polarization state). It has practical potential for application scenarios where system compactness or size requirements are less stringent. However, implementing this approach involves a trade-off as it requires the utilization of additional optical components.

In an in-line digital holography system, as shown in Figure 7c, the object beam is aligned with the reference beam, resulting in a relatively simple and compact optical configuration. The whole field of view is utilized for interfering and a higher-resolution holographic image can be captured. In-line holography generally suffers from the interference of DC term and twin images, which can be partially suppressed by applying a high-pass filter in the frequency domain or employing a phase-shifting strategy.

Gabor holography[123] adapts a slightly different optical schematic, as shown in Figure 7e, compared with typical in-line digital holography configuration (Figure 7d). There is no additional traveling path for the reference light to form holographic fringes. The interference appears between the scattered light from the object and the undisturbed plane reference light, originating from the same light beam. Gabor holography performs a terse layout and provides an effective solution for small object detection[112,113,124–126] and in situ portable devices.

2.3.2. Application of Digital Holography for MPs

Taking advantage of distinct imaging capability, digital holography has been employed in MP analysis, including imaging, detection, identification, quantification, etc. Some application studies are carried out on the reconstructed holograms,[115] while others analyze the raw holographic data directly.[112,114] Reconstruction methods in holography encompass the Fresnel transform and convolution method,[127] as well as the angular spectrum method.[116] These methods involve a series of steps, such as Fourier transform, diffraction propagation calculation, spectrum filtering and shifting, phase unwrapping, and more. In recent years, learning-based methods have emerged, seamlessly incorporating multistep numerical calculations into data-driven automatic parameter fitting.[128–132] They show remarkable improvements in reconstructed image quality and image processing efficiency.[133]

Research on MPs with digital holography can be divided into imaging, quantitative,[134] and qualitative.[135] Based on the imaging environment, applications of digital holography can be categorized into two types: imaging in the air environment and underwater imaging. However, the latter presents more challenges compared to the former, including light scattering, absorption, environmental disturbances, and the requirement for mechanical stability. To address these challenges, researchers employ various strategies such as utilizing phase compensation algorithms and implementing robust holographic recording

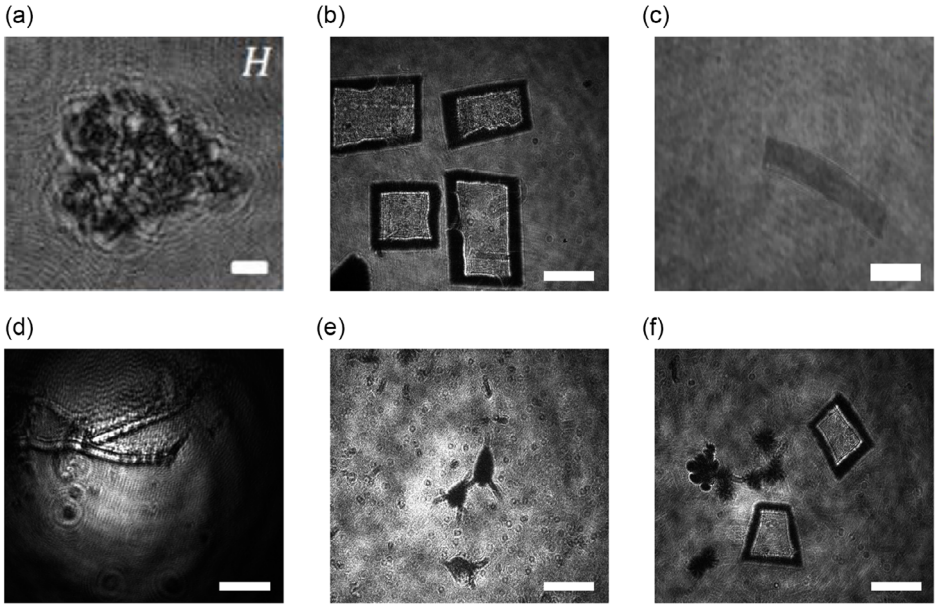

Figure 8. MP imaging with digital holography: a–c) were recorded in the air; (a) adapted under the terms of the CC-BY Creative Commons Attribution 4.0 International license,[120] Copyright 2020, WILEY-VCH Verlag GmbH & Co. KGaA, Weinheim, (b,c) Adapted with permission[31] Copyright 2022, Elsevier B.V.; d–f) were recorded in the water. Scale bar: (a,c) 5 μm; (b,d–f) 0.5 mm.

setups in their systems. **Figure 8** illustrates selected holographic images captured in both air and underwater environments.

Quantitative research primarily focuses on measuring the density or enrichment within a specific volume, as well as the flow rate of particles over a given time period. It typically does not involve identifying specific types of MPs, but rather places emphasis on quantifying the number of particles and particle size. Example research directions include MP pollution assessment,[136] and particle tracking.[124] MP quantification works are conducted both with and without image preprocessing. The former approach involves image reconstruction and denoising, as demonstrated by Zhang et al.[124] (**Figure 9**a). They successfully realized single-particle tracking using a one-stage learning network and 3D particle volumetric reconstruction, showcasing its robustness in analyzing the dynamic displacements and motions of MPs. On the other hand, the latter approach focuses on analyzing the raw holographic images for quantification. In the study showcased in Figure 9b, researchers achieved an accuracy of 97.1% in quantifying MPs within the range of 0–5 particles using a specially designed lightweight network called the holographic-classifier convolutional neural network (HC-CNN). The experimental results demonstrate that HC-CNN can effectively extract image features for accurate MP quantification, even when the resolution of the holographic image is reduced to 128×128 pixels.

Qualitative studies analyze various aspects of MPs, including their categories,[116,120] shapes, textures, and more. These studies encompass the classification of MPs and the direct detection of particles. The former focuses on identifying MP particles based on their characteristics, both among different types of MPs and in relation to natural particles.[31,114] The latter aims to identify and confirm the presence of MPs within an image and mark them out directly.[112] It offers valuable utility for high-throughput MP identification.

Challenges for MP quantification include the difficulty of recording abundant high-resolution images, and the uncertainty of MP characteristics, as they may decompose from large plastic particles and be shaped by natural erosion and aging. To address these challenges, Zhu et al.[113] employed a transfer learning strategy to adapt open-source image data and generalize its features (refer to **Figure 10**a). Moreover, the method achieves a shorter processing time and robust performance utilizing a concatenated rectified linear unit activation and a class-balanced crossentropy loss function. Besides enhancing the image features, additional feature categories, such as semantic attributes, are employed to aid in the classification of MPs. For instance, a zero-shot learning-assisted digital holography system has been developed to characterize MPs, as illustrated in Figure 10b. This method achieves precise identification of MPs by relying on their holographic and morphological character descriptions. It demonstrates to be highly significant in the field of MP detection, particularly in addressing their character uncertainties. As a result, this system extends the classification capability of digital holography beyond known samples to unknown particles and effectively reduces the data requirements associated with learning-based approaches. Furthermore, its applicability can extend to other source-limited tasks involving biological and medical images.

Challenges also exist in MP identification with poor image quality, especially when in field detection. For example, there is image blurring and corruption because of water absorption, turbulent flow, object occlusion, etc.[137] Under such circumstances, the relevant holographic information may be distorted or too weak for the detection and identification of MPs. Image

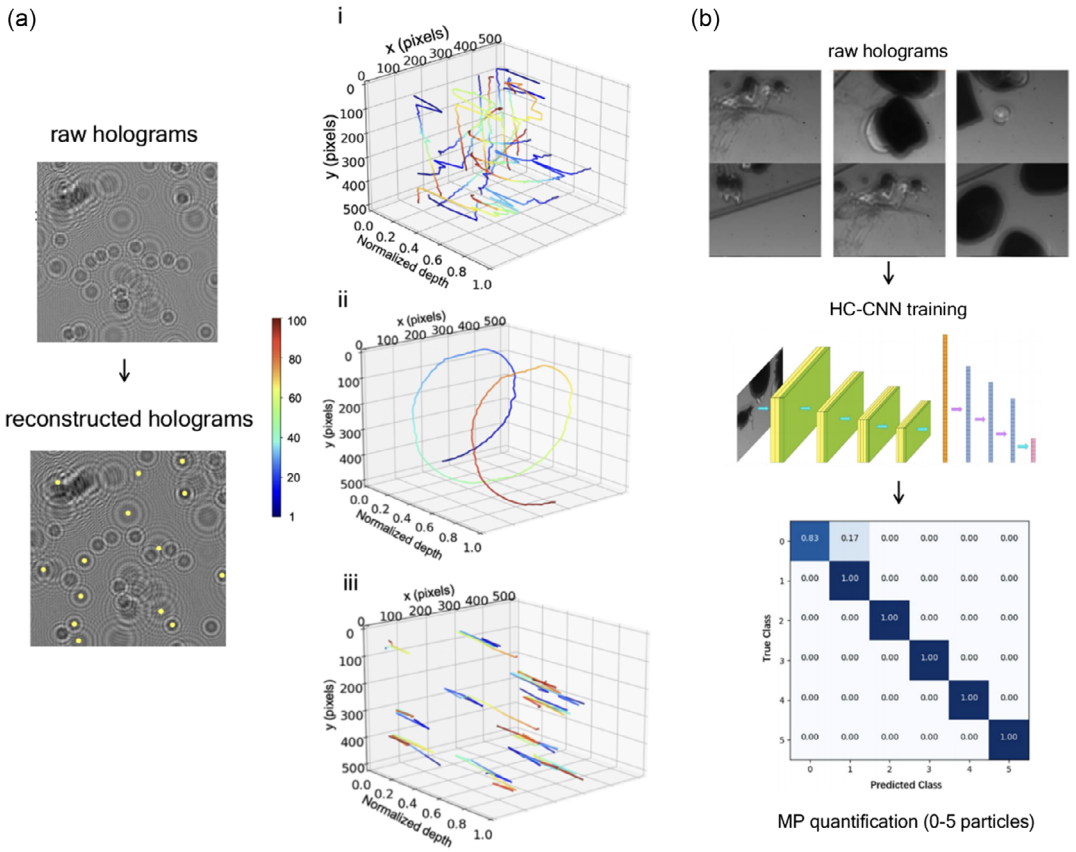

Figure 9. Quantitative analysis on a) MP tracking using digital holography and a one-stage reconstruction network. Adapted under the terms of the CC-BY Creative Commons Attribution 4.0 International license.[124] Copyright 2021, Optica Publishing Group, and b) MP quantification based on raw holographic images. Adapted under the terms of the CC-BY Creative Commons Attribution 4.0 International license.[136] Copyright 2021, IOP Publishing Ltd.

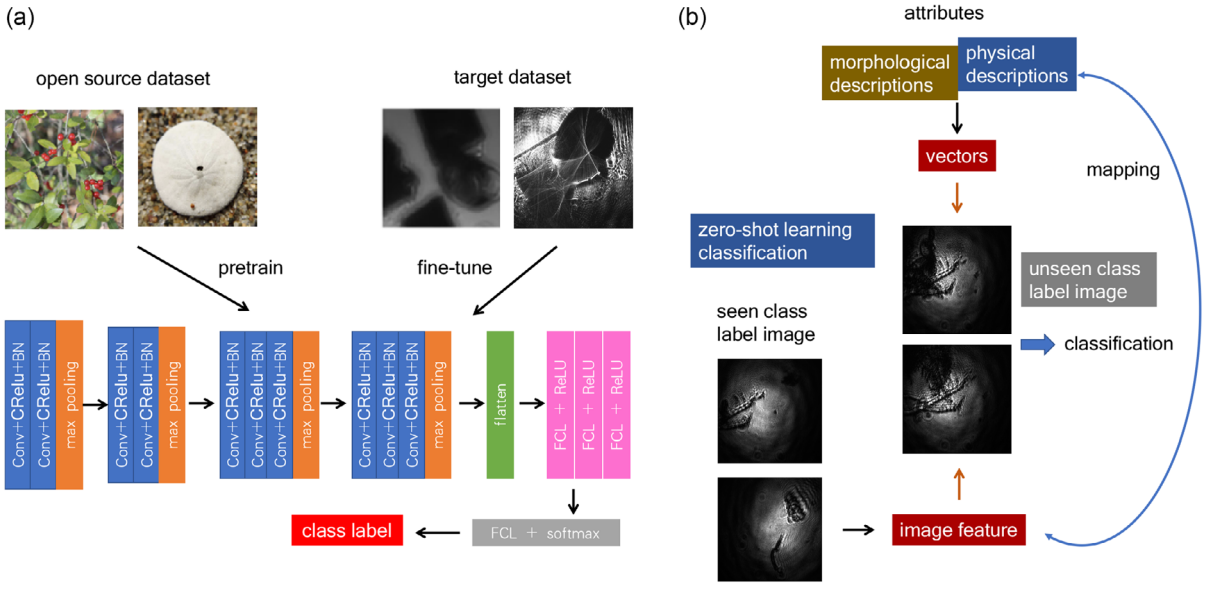

Figure 10. a) Transfer learning-based[113,201] and b) zero-shot learning-based[114] method with digital holography for MP classification.

processing and machine learning methods are adapted to address such problems.[120,132,138] Bianco et al.[120] refocused the recorded holograms, manually extracted the image features, and applied a SVM for feature classification. This method is tested with K-folder cross-validation on liquid samples and achieves over 99% accuracy in classifying thousands of images. Further work[121] investigates the fractal properties of MPs and diatoms. They select multidimensional object fractal properties for MP classification with SVM. This method introduces effective fractal properties that are independent of the sample's shape and make up for blurriness in the images.

Furthermore, digital holography is integrated with other optical systems for material analysis. For instance, Raman spectroscopy[116] and polarized imaging systems[115] are employed, as depicted in **Figure 11**a,b, respectively. Raman spectroscopy measures the intensity of Raman scattering light and captures molecular information,[137] serving as a complementary technique to digital holography for particle material confirmation. Takahashi et al.[116] proposed an integrated Raman and digital holography system that enables simultaneous detection of morphological and chemical information of plastic fragments. This system achieves a comparable detection flow speed of 190 mL s^{-1} with minimal power consumption, showcasing its potential for in situ long-term MP detection. Moreover, the polarization characteristics of plastics are closely related to their surfaces and structures, including factors such as roughness, refractive index, and optical anisotropy. Zhu et al.[108,109] designed a multimodal polarization holography system equipped with a specially designed Stokes polarization mask. This system allows the recording of full polarization state images in a single shot, facilitating quick and noncontact image acquisition. The recorded data provides rich physical information for image analysis and MP identification. It successfully demonstrates the identification of various categories of MPs, including PET, PP, PVC, PC, PS, and PMMA, as well as distinguishing them from other substances such as *Chlorella Magna*, paper, glass, metals, and natural particles. Additionally, Běhal et al.[115] developed a polarization-sensitive digital holography system which is capable of recording holographic information in orthogonal directions. They utilize this system to measure and analyze the orientation of the major axis and the ellipticity angle of different MP fibers. The experimental results demonstrate its ability to identify various plastic categories, including polyamide 6, PET, polyamide 6.6, and PP, as well as distinguishing cotton yarn and wool top.

2.4. Comparison and Discussion

We present a comparison of digital holography, polarization imaging, and hyperspectral imaging in **Table 2**, highlighting their respective capabilities. When light interacts with an MP sample, it undergoes absorption, diffraction, or reflection processes.[139] Imaging systems capture these patterns, enabling the extraction of valuable information regarding the object's structure, surface characteristics, morphology, and material composition. Polarization imaging is particularly effective in revealing material and surface information, while hyperspectral imaging excels at providing material-related insights. Digital holography records both the amplitude and phase information of the object wavefront, enabling the extraction of shape, size, external surface features, and material-related properties of plastics. In summary, digital holography offers a wide range of flexible and versatile detection options, making it a valuable choice for various applications.[140]

2.4.1. Strengths and Limitations

When it comes to sensitivity, digital holography can achieve a lateral resolution of 0.5 µm and an 10 nm axial resolution with additional image processing, such as super-resolution,[131] autofocusing,[88] and reconstruction.[132,141–143] Polarization imaging achieves an accuracy of 0.1–1%, which is defined by the maximum polarization contrast.[144] Hyperspectral imaging, with accurate spectroscopic information, offers a resolution ranging from 0.5 to 10 nm. All three techniques are suitable for accurate MP identification, accommodating variations in surface, shape, material, and morphology of plastic fragments, which interact differently with the incident light. In terms of detectable objects, digital holography excels at imaging transparent and

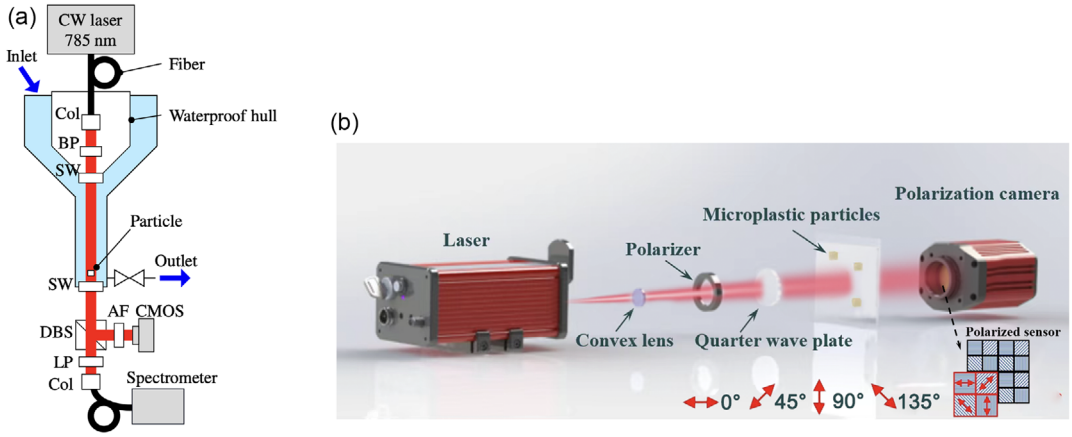

Figure 11. a) Integrated holography and Raman spectroscopy system. Reproduced under the terms of the CC-BY Creative Commons Attribution 4.0 International license.[116] Copyright 2020, The Optical Society; b) polarization-sensitive digital holography system. Reproduced with permission.[109] Copyright 2023, Society of Photo-Optical Instrumentation Engineers (SPIE).

Table 2. Comparison of digital holography, polarization imaging, and hyperspectral imaging.

Imaging technology	Digital holography	Polarization imaging	Hyperspectral imaging
Detectable characters	• Shape • Size • Material • Surface	• Material • Surface	• Shape • Size • Material
Particle detectable sensitivity	• ≈100 nm	• 1 − 10 μm [144]	• 0.5–10 nm
Preference MP category	• Transparent • Semitransparent	• Semitransparent • Opaque	• Semitransparent • Opaque
Current application stage	• Air • In the water	• Air	• Air
Efficiency	• High (one-shot imaging) • moderate (scanning recording)	• High (with polarization camera) • Low (manual polarization state adjustment)	• Low (spectrum processing)
Cost	• Low • (>USD 500)	• Moderate • (>USD 4000)[145]	• High (>USD 10 000)[147]
Limitation	• Weak for opaque MPs.	• Need polarization state control of light source.	• Slow with spectrum processing.

semitransparent MPs. Polarization imaging and hyperspectral imaging are well-suited for imaging semitransparent and opaque MPs. Considering the experimental environment, digital holography has successfully detected small plastics in both air and underwater settings. Polarization imaging and hyperspectral imaging have been employed in lab settings for MP detection and hold potential for field applications. In terms of imaging efficiency, digital holography offers high efficiency with one-shot image recording, while also providing holographic fringes at different thicknesses through lateral scanning. Polarization imaging typically relies on manual rotation of linear polarizers to generate polarization images, which is relatively slower compared to one-shot and automatic image recording. However, recent advancements in polarization cameras with specially manufactured masks[107,108] offer a high-speed alternative. Regarding experimental cost, digital holography presents a relatively low-cost option with its lensless and compact setups, as depicted in Figure 7. On the other hand, an advanced polarization camera for polarization imaging can cost around USD 2500[145] to 25 000.[146] Hyperspectral imaging incurs higher costs, with camera systems ranging from USD 10 000 to 15 000[147] and laboratory-grade cameras ranging from USD 30 000 to 100 000[148] or more. As for limitations, digital holography records limited information for opaque MPs, but a reflective system setup can aid in image recording. Polarization imaging systems require accurate polarization state control to capture distinct sample information. Hyperspectral imaging is relatively slower due to the need for spectrum recording, impacting imaging speed.

2.4.2. Prospects and Challenges

Portable digital holography devices have emerged as a promising direction for in situ detection and identification of MPs, offering notable advantages such as affordability, rapid detection, and user-friendly operation. These devices incorporate computational hardware that enables fast data processing and transmission. They are designed for both underwater and airborne detection.[117–119,149] The key components include a source, the sample channel, and the image recording, as depicted in **Figure 12**. In the source, low-cost and energy-efficient options, such as laser diodes and battery-charged lasers, are commonly employed, and additional optical devices for light collimation, such as pinholes,[150] objectives, aspheric lenses,[149] relay lenses, and specially-designed lenses,[151] can be integrated. The image recording houses a sensor and onboard computational hardware such as Raspberry Pi[118] or commercial off-the-shelf (COTS) computers.[149] A sampling channel, typically several centimeters wide, facilitates sample placement or flow for image acquisition. To ensure device integrity and protection against environmental interference, an external enclosure is included.

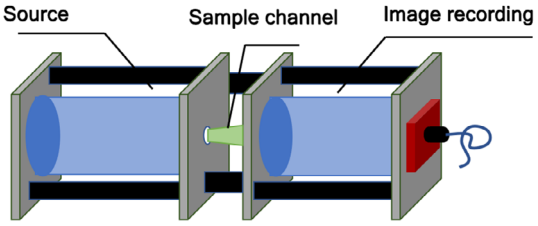

Figure 12. The general framework of the portable digital holography device consists of three components: the source, the sample channel, and the image recording. This setup enables compact and mobile holographic imaging.

Portable devices are often enhanced by integrating additional hardware for specific applications. For instance, Dyomin et al.[152] developed a submersible digital holographic camera, depicted in **Figure 13**a, to investigate the vertical plankton distribution in Lake Baikal. The digital holographic microscope system LISST-Holo2, shown in Figure 13b, is equipped with an autonomous drone for measuring coastal MPs.[119] Furthermore, Ramirez et al.[117] mounted pressure and temperature sensors onto a digital holographic microscope, which was deployed on a BlueRov2 robot for in situ microbial imaging in underwater environments. Mallery et al.[118] designed a robotic platform called Aquapod, enabling operations in challenging terrains such as snowy, sandy, and muddy conditions.

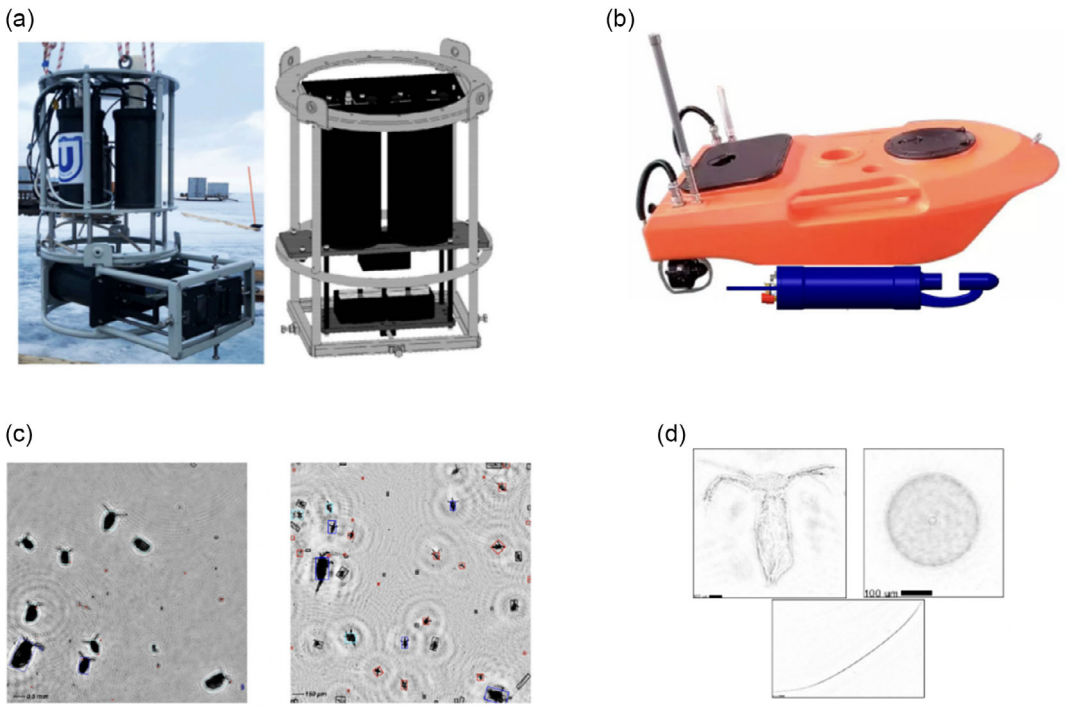

Figure 13. Portable device demonstration: a) Submersible digital holographic camera horizontal and vertical layout. Adapted under the terms of the CC-BY Creative Commons Attribution 4.0 International license.[152] Copyright 2020, Frontiers. b) LISST-Holo2[119] mounted on a marine drone. Adapted under the terms of the CC-BY Creative Commons Attribution 4.0 International license.[119] Copyright 2022, MDPI, Basel, Switzerland. c,d) are identification results based on the holographic images captured by (a) and (b).

The practical application of portable imaging devices for in situ identification of MP still faces certain limitations. One is the relatively low sensitivity and resolution compared to lab-based imaging systems, which affects their performance in detecting tiny and low-concentration MPs. Additionally, when testing in large sample volumes, they may yield unsatisfactory results due to insufficient light intensity. They are also susceptible to environmental influences, leading to errors in system calibration. Moreover, portable devices can generate substantial amounts of data that pose challenges in terms of real-time analysis and interpretation.

Currently, portable devices are capable of measuring particle size, shape, refractive index, and concentration, which can be utilized for particle detection, quantification, and tracking. However, for accurate and reliable identification, it is often necessary to register most of the measurement results with in-lab confirmation. From a hardware perspective, further advancements in in situ devices can be made by incorporating stable and powerful light sources to ensure clear image acquisition, especially in underwater environments where light intensity is attenuated by water absorption and scattering. Multimodal imaging devices, such as integrated systems combining Raman spectroscopy, digital holography, and polarization imaging, offer a comprehensive and multidimensional approach for discriminative material analysis and sample identification.[109] Additionally, the integration of microfluidic devices or flow control devices enables high-throughput particle tracking, counting, and classification.[153,154] Finally, the incorporation of 3D-printed stabilizers facilitates measurements in flowing water, enhancing the stability and accuracy of the device.

3. Conclusion and Prospect

MP pollutants have emerged as a significant global environmental concern, leading to the development and application of various detection methods. These methods encompass imaging-based, thermal, and chemical analysis techniques.[27,78,155] Practical MP detection often necessitates the utilization of multiple methods to ensure reliable results.[156,157] By combining thermal and chemical techniques with imaging-based methods, a more comprehensive approach to MP detection can be achieved. A crucial objective is the identification and quantification of MP particles, alongside their chemical compositions and size distributions.[158] Researchers have explored the coupling of pyrolysis–GC–MS with TEM–EDX to investigate MPs within compost and soil fractions, providing insights from both morphological and analytical perspectives.[70] Furthermore, the integration of FTIR and Raman spectroscopy with light microscopes, known as μ-FTIR and μ-Raman, respectively, enables noninvasive examination of very small specimens or features.[159,160]

However, these methods face several challenges,[161] such as MPs being present in complex matrices, making it difficult to

distinguish them from natural particles. Moreover, the varying shapes and sizes of MPs can make distinguishing them from natural particles difficult, especially for small MPs below −10 μm in size.[155] False positives can also occur due to the presence of other small particles or debris in the sample.[162,163] Additionally, some detection methods can be expensive and require specialized training and facilities.

To address these challenges, future MP detection could be further developed in the following directions. First, the integration of different detection methods, such as spectroscopic and imaging techniques, can improve the accuracy and reliability of MP detection.[159,164] Second, the development of standardized methods for sample collection, preparation, and analysis can help to improve the comparability of results across different studies and regions.[22] Third, automating detection methods could increase efficiency and reduce costs.[112] Furthermore, the development of portable and low-cost detection devices could make MP detection more accessible, particularly in remote or low-resource areas.[118] Finally, the development of more sensitive and selective detection methods could improve the ability to ensure the accurate and reliable detection of MPs and reduce false positives.[165]

In recent years, the field of MPs detection has witnessed the application of several emerging imaging techniques.[166,167] These techniques offer valuable insights for MP identification and analysis, potentially shedding light on the distribution and impact of MPs in the environment. One notable approach involves the combination of neutron and X-Ray tomography for the detection of MP particles in sandy sediments.[168] This synergistic utilization of both techniques ensures high sensitivity and robustness, enabling the detection of even small MP particles with a spatial resolution of less than 100 μm. An additional advantage of this method is its nondestructive sample preparation, allowing for the analysis of sediment and soil microstructure with excellent contrast. Furthermore, flow cytometry (FlowCam) has proven effective in detecting and analyzing MPs in water samples.[169,170] This technique combines high-resolution imaging with flow cytometry, capturing images of particles as they flow through a specialized cell. The acquired images are subsequently analyzed to determine the size, shape, and composition of the particles. FlowCam is particularly advantageous in complex environmental samples such as seawater and wastewater, where the presence of MPs can be detected and characterized.

Emerging advanced sensors and optical devices, including metasurface devices,[171,172] quanta imaging sensors (QIS),[173] neuromorphic cameras,[174–177] and single-photon avalanche diodes (SPAD) arrays,[178,179] exhibit remarkable imaging capabilities. These cutting-edge hardware advancements offer innovative possibilities for the development of imaging systems dedicated to MP detection. For instance, event cameras hold the potential for high-throughput MP tracking and localization, enabling efficient and precise monitoring. In low-light conditions, such as during nighttime or in foggy and rainy environments, QIS proves valuable for MP detection.[180] SPAD cameras present an effective solution for the 3D reconstruction and profiling of MPs, enhancing the accuracy and depth of analysis. Furthermore, by incorporating metasurfaces into polarization cameras, the polarization state of light can be modulated at various angles. This integrated system allows for the recording of polarized holograms with desired polarization states, enabling precise polarization MP imaging configurations.

Machine learning and artificial intelligence techniques have made significant advancements in recent years.[181] In the realm of computational imaging, they have proven successful in various applications such as image reconstruction,[182,183] resolution enhancement, image rendering, object detection,[184] and tracking.[185] Supervised and unsupervised learning methods have the potential to overcome the limitations of optical hardware and image processing technologies, offering promising solutions for imaging tasks. For low-level imaging tasks like super-resolution, phase retrieval,[142,186] autofocusing, extending the field of view,[187] and image reconstruction, decoding–encoding network structures,[141] generative networks,[188] metalearning,[189] zero-/few-shot learning, transfer learning, and model-informed networks[107,190] have provided substantial support. Furthermore, artificial intelligence demonstrates notable performance in high-level tasks. For instance, one-stage and two-stage object recognition methods[191] enable sample detection and tracking. Attention mechanisms and transformer models facilitate image style transfer[192] and crosscategory registration.[193] Classification structures contribute to image identification, while derivative networks aid in image system co-optimization.[194]

In the field of MP research, artificial intelligence has found applications in various areas such as category classification,[113,195] material identification,[120] rapid detection,[112,196] pollution assessment,[114] and toxicity analysis.[68] However, there are several aspects where further development and consideration are needed. First, the identification of MP can be enhanced through the integration and fusion of multimodal imaging systems, addressing potential confusion and improving accuracy. Additionally, robust discrimination of different materials constituting MPs is an ongoing challenge that requires further advancements in optical technologies. Furthermore, in situ detection scenarios present complexity due to environmental interferences such as water turbulence,[197] light scattering from floating particles, and attenuation of the light source. Overcoming these challenges and achieving precise and reliable material identification remain an area of continuous exploration and improvement in optical technologies.[198] Moreover, there is a need for the development of in situ high-speed detection methods and high-resolution imaging techniques capable of operating in extreme environments. These advancements would enable a more efficient and accurate assessment of MP's presence and characteristics.

Acknowledgements

Y.Z. and Y.L. contributed equally to this work. The work was supported in part by the Research Grants Council of Hong Kong (GRF 17201620 and RIF R7003-21). This work was partly funded by the Hong Kong Scholars Program (XJ2022032). J.H. appreciates the partial financial support from Shanghai Jiao Tong University.

Conflict of Interest

The authors declare no conflict of interest.

Author Contributions

Yanmin Zhu: Conceptualization (equal); Writing – original draft (lead); Writing – review and editing:(lead). **Yuxing Li**: Conceptualization (equal); Writing – original draft (lead); Writing – review and editing (lead). **Jianqing Huang**: Conceptualization (equal); Writing – original draft (equal); Writing – review and editing (lead). **Yunping Zhang**: Conceptualization (equal); Writing – original draft (equal); Writing – review and editing (lead). **Yuen-Wa Ho**: Writing – review and editing (supporting). **James Kar-Hei Fang**: Review and editing (supporting). **Edmund Y. Lam**: Conceptualization (lead); Funding acquisition (lead); Resources (lead); Supervision (lead); Writing – review and editing (lead).

Keywords

microplastics detections, optical imaging technologies, pollution monitoring, portable devices

Received: March 8, 2024
Revised: June 22, 2024
Published online: July 22, 2024

[1] R. C. Thompson, Y. Olsen, R. P. Mitchell, A. Davis, S. J. Rowland, A. W. G. John, D. McGonigle, A. E. Russell, *Science* **2004**, *304*, 838.
[2] X. Wang, N. Bolan, D. C. W. Tsang, B. Sarkar, L. Bradney, Y. Li, *J. Hazard. Mater.* **2021**, *402*, 123496.
[3] C. Guerranti, T. Martellini, G. Perra, C. Scopetani, A. Cincinelli, *Environ. Toxicol. Pharmacol.* **2019**, *68*, 75.
[4] T. Liang, Z. Lei, M. T. I. Fuad, Q. Wang, S. Sun, J. K.-H. Fang, X. Liu, *Sci. Total Environ.* **2022**, *806*, 150526.
[5] A. Chamas, H. Moon, J. Zheng, Y. Qiu, T. Tabassum, J. H. Jang, M. Abu-Omar, S. L. Scott, S. Suh, *ACS Sustainable Chem. Eng.* **2020**, *8*, 3494.
[6] M. Capolupo, L. Sørensen, K. D. R. Jayasena, A. M. Booth, E. Fabbri, *Water Res.* **2020**, *169*, 115270.
[7] Y.-Q. Zhang, M. Lykaki, M. T. Alrajoula, M. Markiewicz, C. Kraas, S. Kolbe, K. Klinkhammer, M. Rabe, R. Klauer, E. Bendt, S. Stolte, *Green Chem.* **2021**, *23*, 5247.
[8] J. M. Goncalves, M. J. Bebianno, *Environ. Pollut.* **2021**, *273*, 116426.
[9] A. G. Anderson, J. Grose, S. Pahl, R. C. Thompson, K. J. Wyles, *Mar. Pollut. Bull.* **2016**, *113*, 454.
[10] J. R. Jambeck, R. Geyer, C. Wilcox, T. R. Siegler, M. Perryman, A. Andrady, R. Narayan, K. L. Law, *Science* **2015**, *347*, 768.
[11] E. Van Sebille, C. Wilcox, L. Lebreton, N. Maximenko, B. D. Hardesty, J. A. van Franeker, M. Eriksen, D. Siegel, F. Galgani, K. L. Law, *Environ. Res. Lett.* **2015**, *10*, 124006.
[12] V. Castelvetro, A. Corti, S. Bianchi, A. Ceccarini, A. Manariti, V. Vinciguerra, *J. Hazard. Mater.* **2020**, *385*, 121517.
[13] A. D. Vethaak, J. Legler, *Science* **2021**, *371*, 672.
[14] C. Campanale, C. Massarelli, I. Savino, V. Locaputo, V. F. Uricchio, *Int. J. Environ. Res. Public Health* **2020**, *17*, 1212.
[15] K. L. Law, R. C. Thompson, *Science* **2014**, *345*, 144.
[16] J. Wang, X. Qin, J. Guo, W. Jia, Q. Wang, M. Zhang, Y. Huang, *Water Res.* **2020**, *183*, 116113.
[17] L. Frère, L. Maignien, M. Chalopin, A. Huvet, E. Rinnert, H. Morrison, S. Kerninon, A.-L. Cassone, C. Lambert, J. Reveillaud, I. Paul-Pont, *Environ. Pollut.* **2018**, *242*, 614.
[18] T. S. Galloway, C. N. Lewis, *Proc. Natl. Acad. Sci. USA* **2016**, *113*, 2331.
[19] X. Liu, C. Liang, M. Zhou, Z. Chang, L. Li, *Ecotoxicol. Environ. Saf.* **2023**, *249*, 114377.
[20] M. N. Issac, B. Kandasubramanian, *Environ. Sci. Pollut. Res.* **2021**, *28*, 19544.
[21] L. Wan, H. Cheng, Y. Liu, Y. Shen, G. Liu, X. Su, *Sci. Total Environ.* **2023**, *867*, 161403.
[22] W. Fu, J. Min, W. Jiang, Y. Li, W. Zhang, *Sci. Total Environ.* **2020**, *721*, 137561.
[23] W. Li, Y. Luo, X. Pan, in *The Handbook of Environmental Chemistry*, Springer, New York **2020**, pp. 25–37.
[24] A. S. Tagg, M. Sapp, J. P. Harrison, J. J. Ojeda, *Anal. Chem.* **2015**, *87*, 6032.
[25] M. M.-L. Leung, Y.-W. Ho, C.-H. Lee, Y. Wang, M. Hu, K. W. H. Kwok, S.-L. Chua, J. K.-H. Fang, *Environ. Pollut.* **2021**, *289*, 117648.
[26] J. Barrett, Z. Chase, J. Zhang, M. M. B. Holl, K. Willis, A. Williams, B. D. Hardesty, C. Wilcox, *Front. Marine Sci.* **2020**, 808.
[27] M. Fischer, B. M. Scholz-Böttcher, *Anal. Methods* **2019**, *11*, 2489.
[28] P. Eisentraut, E. Dümichen, A. S. Ruhl, M. Jekel, M. Albrecht, M. Gehde, U. Braun, *Environ. Sci. Technol. Lett.* **2018**, *5*, 608.
[29] F. Stock, C. Kochleus, B. Bänsch-Baltruschat, N. Brennholt, G. Reifferscheid, *Trends Anal. Chem.* **2019**, *113*, 84.
[30] A. Faltynkova, G. Johnsen, M. Wagner, *Microplast. Nanoplast.* **2021**, *1*, 1.
[31] M. Valentino, J. Běhal, V. Bianco, S. Itri, R. Mossotti, G. Dalla Fontana, T. Battistini, E. Stella, L. Miccio, P. Ferraro, *Sci. Total Environ.* **2022**, *815*, 152708.
[32] A. Baruah, A. Sharma, S. Sharma, R. Nagraik, *Int. J. Environ. Sci. Technol.* **2022**, *19*, 5721.
[33] W. J. Shim, S. H. Hong, S. E. Eo, *Anal. Methods* **2017**, *9*, 1384.
[34] H. W. Schreier, D. Garcia, M. A. Sutton, *Exp. Mech.* **2004**, *44*, 278.
[35] W.-H. Liao, S. J. Aggarwal, J. K. Aggarwal, *Mach. Vis. Appl.* **1997**, *9*, 166.
[36] M. Lee, G. Gibson, D. Phillips, M. Padgett, M. Tassieri, *Opt. Express* **2014**, *22*, 4671.
[37] R. Mossotti, G. Dalla Fontana, A. Anceschi, E. Gasparin, T. Battistini, in *Advances and Challenges in Microplastics*, IntechOpen Limited, London **2023**.
[38] J. S. Hanvey, P. J. Lewis, J. L. Lavers, N. D. Crosbie, K. Pozo, B. O. Clarke, *Anal. Methods* **2017**, *9*, 1369.
[39] N. B. Nguyen, M.-K. Kim, Q. T. Le, D. N. Ngo, K.-D. Zoh, S.-W. Joo, *Chemosphere* **2021**, *263*, 127812.
[40] M. L. Kalnasa, S. M. O. Lantaca, L. C. Boter, G. J. T. Flores, R. G. Van Ryan Kristopher, *Mar. Pollut. Bull.* **2019**, *149*, 110521.
[41] R. Pashaei, S. A. Loiselle, G. Leone, G. Tamasi, R. Dzingelevičienė, T. Kowalkowski, M. Gholizadeh, M. Consumi, S. Abbasi, V. Sabaliauskaitė, B. Buszewski, *Environ. Monit. Assess.* **2021**, *193*, 668.
[42] Y. K. Song, S. H. Hong, M. Jang, G. M. Han, M. Rani, J. Lee, W. J. Shim, *Mar. Pollut. Bull.* **2015**, *93*, 202.
[43] M. Eriksen, S. Mason, S. Wilson, C. Box, A. Zellers, W. Edwards, H. Farley, S. Amato, *Mar. Pollut. Bull.* **2013**, *77*, 177.
[44] V. H. da Silva, F. Murphy, J. M. Amigo, C. Stedmon, J. Strand, *Anal. Chem.* **2020**, *92*, 13724.
[45] M. J. Sanderson, I. Smith, I. Parker, M. D. Bootman, *Cold Spring Harb. Protoc.* **2014**, *2014*, pdb–top071795.
[46] I. C. Ghiran, in *Light Microscopy: Methods and Protocols*, Humana Totowa, NJ **2011**, pp. 93–136.
[47] M. Klein, E. K. Fischer, *Sci. Total Environ.* **2019**, *685*, 96.
[48] S. Dehghani, F. Moore, R. Akhbarizadeh, *Environ. Sci. Pollut. Res.* **2017**, *24*, 20360.
[49] D. Kankanige, S. Babel, *J. Water Process Eng.* **2021**, *40*, 101765.
[50] C. Stewart, J. Giannini, *J. Chem. Educ.* **2016**, *93*, 1310.
[51] I. Sase, H. Miyata, J. Corrie, J. S. Craik, K. Kinosita Jr., *Biophys. J.* **1995**, *69*, 323.
[52] J. C. Stockert, A. Blázquez-Castro, in *Fluorescence Microscopy in Life Sciences*, Bentham Science Publishers, Sharjah, UAE **2017**.
[53] L. Li, Y. Luo, W. J. Peijnenburg, R. Li, J. Yang, Q. Zhou, *MethodsX* **2020**, *7*, 100750.

[54] T. Takahashi, K. P. Herdzik, K. N. Bourdakos, J. A. Read, S. Mahajan, *Anal. Chem.* **2021**, *93*, 5234.
[55] F. Norén, Small Plastic Particles in Coastal Swedish Waters, KIMO, Sweden **2007**.
[56] A. Scircle, J. V. Cizdziel, *J. Chem. Educ.* **2019**, *97*, 234.
[57] J. Leonard, H. C. Koydemir, V. S. Koutnik, D. Tseng, A. Ozcan, S. K. Mohanty, *Mater. Lett.* **2022**, *3*, 100052.
[58] D. Kalaronis, N. M. Ainali, E. Evgenidou, G. Z. Kyzas, X. Yang, D. N. Bikiaris, D. A. Lambropoulou, *Green Anal. Chem.* **2022**, 100036.
[59] Y. K. Lee, K. R. Murphy, J. Hur, *Environ. Sci. Technol.* **2020**, *54*, 11905.
[60] C. N. Afzulpurkar, et al., *Ph.D. Thesis,* University of Texas Arlington, **2021**.
[61] K. Akhtar, S. A. Khan, S. B. Khan, A. M. Asiri, in *Handbook of Materials Characterization*, Springer, Cham **2018**, pp. 113–145.
[62] Z.-M. Wang, J. Wagner, S. Ghosal, G. Bedi, S. Wall, *Sci. Total Environ.* **2017**, *603*, 616.
[63] I. Sekudewicz, A. M. Dabrowska, M. D. Syczewski, *Sci. Total Environ.* **2021**, *762*, 143111.
[64] L. Cai, J. Wang, J. Peng, Z. Tan, Z. Zhan, X. Tan, Q. Chen, *Environ. Sci. Pollut. Res.* **2017**, *24*, 24928.
[65] X. Luo, Z. Wang, L. Yang, T. Gao, Y. Zhang, *Sci. Total Environ.* **2022**, 154487.
[66] E. Fries, J. H. Dekiff, J. Willmeyer, M.-T. Nuelle, M. Ebert, D. Remy, *Environ. Sci.: Process. Impacts* **2013**, *15*, 1949.
[67] M. Han, X. Niu, M. Tang, B.-T. Zhang, G. Wang, W. Yue, X. Kong, J. Zhu, *Sci. Total Environ.* **2020**, *707*, 135601.
[68] T. Ishida, T. Owaki, M. Ohtsuka, M. Kuwahara, K. Saitoh, T. Kawasaki, *Appl. Phys. Express* **2022**, *15*, 115001.
[69] Q. Tian, H. Luo, R. Yi, X. Fan, Y. Ma, D. Shi, J. Gao, *Mater. Sci. Eng. A* **2020**, *771*, 138645.
[70] F. Watteau, M.-F. Dignac, A. Bouchard, A. Revallier, S. Houot, *Front. Sustain. Food Syst.* **2018**, *2*, 81.
[71] F. J. Giessibl, *Rev. Mod. Phys.* **2003**, *75*, 949.
[72] G. Binnig, C. F. Quate, C. Gerber, *Phys. Rev. Lett.* **1986**, *56*, 930.
[73] B. Cappella, G. Dietler, *Surf. Sci. Rep.* **1999**, *34*, 1.
[74] T. Sulchek, R. Hsieh, J. Adams, S. Minne, C. Quate, D. Adderton, *Rev. Sci. Instrum.* **2000**, *71*, 2097.
[75] Y. Li, C. Zhang, Z. Tian, X. Cai, B. Guan, *J. Hazard. Mater.* **2024**, *463*, 132933.
[76] S. Cheng, R. Bryant, S. H. Doerr, C. J. Wright, P. R. Williams, *Environ. Sci. Technol.* **2009**, *43*, 6500.
[77] W. Fu, W. Zhang, *Small* **2017**, *13*, 1603525.
[78] S. Mariano, S. Tacconi, M. Fidaleo, M. Rossi, L. Dini, *Front. Toxicol.* **2021**, *3*, 636640.
[79] F. Akhatova, I. Ishmukhametov, G. Fakhrullina, R. Fakhrullin, *Int. J. Mol. Sci.* **2022**, *23*, 806.
[80] P. Melo-Agustn, E. R. Kozak, M. de Jesús Perea-Flores, J. A. Mendoza-Pérez, *Sci. Total Environ.* **2022**, *828*, 154434.
[81] H. Luo, Y. Xiang, Y. Zhao, Y. Li, X. Pan, *Sci. Total Environ.* **2020**, *744*, 140944.
[82] M. Gniadek, A. Dabrowska, *Mar. Pollut. Bull.* **2019**, *148*, 210.
[83] A. V. Girão, in *Handbook of Microplastics in the Environment*, Springer, Cham **2020**, pp. 1–22.
[84] J. Caldwell, C. Loussert-Fonta, G. Toullec, N. Heidelberg Lyndby, B. Haenni, P. Taladriz-Blanco, B. Espiña, B. Rothen-Rutishauser, A. Petri-Fink, *Environ. Sci. Technol.* **2023**, *57*, 6664.
[85] T. E. Davies, H. Li, S. Bessette, R. Gauvin, G. S. Patience, N. F. Dummer, *Can. J. Chem. Eng.* **2022**, *100*, 3145.
[86] R. J. Cannara, M. Eglin, R. W. Carpick, *Rev. Sci. Instrum.* **2006**, *77*, 053701.
[87] H. Grahn, P. Geladi, in *Techniques and Applications of Hyperspectral Image Analysis*, John Wiley & Sons, Hoboken, NJ **2007**.
[88] Z. Ren, Z. Xu, E. Lam, *Optica* **2018**, *5*, 337.
[89] M. Paturzo, V. Pagliarulo, V. Bianco, P. Memmolo, L. Miccio, F. Merola, P. Ferraro, *Opt. Lasers Eng.* **2018**, *104*, 32.
[90] G. A. Roth, S. Tahiliani, N. M. Neu-Baker, S. A. Brenner, *Wiley Interdiscip. Rev.: Nanomed. Nanobiotechnol.* **2015**, *7*, 565.
[91] J. Shan, J. Zhao, Y. Zhang, L. Liu, F. Wu, X. Wang, *Anal. Chim. Acta* **2019**, *1050*, 161.
[92] M. Hu, Z. Wu, Q. Huang, X. Yuan, D. Brady, *Intell. Comput.* **2023**, *2*, 0038.
[93] X. Yuan, D. J. Brady, A. K. Katsaggelos, *IEEE Signal Process. Mag.* **2021**, *38*, 65.
[94] H. Huang, J. U. Qureshi, S. Liu, Z. Sun, C. Zhang, H. Wang, *Bull. Environ. Contam. Toxicol.* **2021**, *107*, 754.
[95] S. Serranti, R. Palmieri, G. Bonifazi, A. Cózar, *Waste Manage.* **2018**, *76*, 117.
[96] C. Zhu, Y. Kanaya, R. Nakajima, M. Tsuchiya, H. Nomaki, T. Kitahashi, K. Fujikura, *Environ. Pollut.* **2020**, *263*, 114296.
[97] S. Piarulli, G. Sciutto, P. Oliveri, C. Malegori, S. Prati, R. Mazzeo, L. Airoldi, *Chemosphere* **2020**, *260*, 127655.
[98] J. Shan, J. Zhao, L. Liu, Y. Zhang, X. Wang, F. Wu, *Environ. Pollut.* **2018**, *238*, 121.
[99] T. M. Karlsson, H. Grahn, B. van Bavel, P. Geladi, *J. Near Infrared Spectrosc.* **2016**, *24*, 141.
[100] Y. Zhang, X. Wang, J. Shan, J. Zhao, W. Zhang, L. Liu, F. Wu, *Environ. Sci. Technol.* **2019**, *53*, 5151.
[101] R. Gong, J. Wang, X. Wang, Y. Liu, J. Shan, *Food Packag. Shelf Life* **2023**, *39*, 101152.
[102] I. CytoViva, CytoViva: Hyperspectral Microscope **2022**, https://www.cytoviva.com/cytoviva-hyperspectral-microscope (accessed: 2022).
[103] M. J. Gallagher, J. T. Buchman, T. A. Qiu, B. Zhi, T. Y. Lyons, K. M. Landy, Z. Rosenzweig, C. L. Haynes, D. H. Fairbrother, *Environ. Sci.: Nano* **2018**, *5*, 1694.
[104] H. Huang, Z. Sun, S. Liu, Y. Di, J. Xu, C. Liu, R. Xu, H. Song, S. Zhan, J. Wu, *Sci. Total Environ.* **2021**, *776*, 145960.
[105] S. Tominaga, A. Kimachi, *Opt. Eng.* **2008**, *47*, 123201.
[106] I. Sierra, M. R. Chialanza, R. Faccio, D. Carrizo, L. Fornaro, A. Pérez-Parada, *Environ. Sci. Pollut. Res.* **2020**, *27*, 7409.
[107] Y. Zhu, T. Zeng, K. Liu, Z. Ren, E. Y. Lam, *Opt. Express* **2021**, *29*, 41865.
[108] Y. Zhu, Y. Li, J. Huang, Y. Zhang, E. Y. Lam, in *Computational Optical Sensing and Imaging*, Optica Publishing Group, NW Washington, DC **2023**, p. JW2A.3.
[109] Y. Zhu, Y. Li, J. Huang, Y. Zhang, E. Y. Lam, in *Multimodal Sensing and Artificial Intelligence: Technologies and Applications III* Vol. *12621*, SPIE, Bellingham, Washington **2023**, pp. 234–236.
[110] A. B. Labbe, C. R. Bagshaw, L. Uttal, *J. Chem. Educ.* **2020**, *97*, 4026.
[111] J. W. Goodman, in *Introduction to Fourier Optics*, 4th ed., W. H. Freeman, New York, NY **2017**.
[112] Y. Zhu, C. H. Yeung, E. Y. Lam, in *Digital Holography and Three-Dimensional Imaging*, Optica Publishing Group, NW Washington, DC **2020**, p. HTu5B–1.
[113] Y. Zhu, C. H. Yeung, E. Y. Lam, *Appl. Opt.* **2021**, *60*, A38.
[114] Y. Zhu, H. K. A. Lo, C. H. Yeung, E. Y. Lam, *APL Photonics* **2022**, *7*, 076102.
[115] J. Běhal, M. Valentino, L. Miccio, V. Bianco, S. Itri, R. Mossotti, G. Dalla Fontana, E. Stella, P. Ferraro, *ACS Photonics* **2022**, *9*, 694.
[116] T. Takahashi, Z. Liu, T. Thevar, N. Burns, S. Mahajan, D. Lindsay, J. Watson, B. Thornton, *Appl. Opt.* **2020**, *59*, 5073.
[117] A. Ramirez, T. Burch, J. K. Wallace, in *2022 IEEE Aerospace Conf. (AERO)*, IEEE, Piscataway, NJ **2022**, pp. 1–7.
[118] K. Mallery, D. Canelon, J. Hong, N. Papanikolopoulos, *J. Intell. Robot. Syst.* **2021**, *102*, 32.
[119] D. Calore, N. Fraticelli, *Microplastics* **2022**, *1*, 640.

[120] V. Bianco, P. Memmolo, P. Carcagn, F. Merola, M. Paturzo, C. Distante, P. Ferraro, *Adv. Intell. Syst.* **2020**, *2*, 1900153.
[121] V. Bianco, D. Pirone, P. Memmolo, F. Merola, P. Ferraro, *ACS Photonics* **2021**, *8*, 2148.
[122] M. K. Kim, *SPIE Rev.* **2010**, *1*, 018005.
[123] D. Gabor, *Nature* **1948**, *161*, 777.
[124] Y. Zhang, Y. Zhu, E. Y. Lam, *Appl. Opt.* **2022**, *61*, B111.
[125] J. Huang, Z. Wu, W. Cai, E. Berrocal, M. Aldén, Z. Li, *Powder Technol.* **2022**, *405*, 117554.
[126] J. Huang, Z. Wu, W. Cai, E. Berrocal, M. Aldén, Z. Li, *Powder Technol.* **2023**, *420*, 118412.
[127] C. Liu, D. Wang, Y. Zhang, *Opt. Eng.* **2009**, *48*, 105802.
[128] Z. Ren, Z. Xu, E. Y. Lam, *Photonics* **2019**, *1*, 016004.
[129] H. Wang, M. Lyu, G. Situ, *Opt. Express* **2018**, *26*, 22603.
[130] Z. Ren, T. Zeng, E. Y. Lam, in *Computational Optical Sensing and Imaging*, Optica Publishing Group, NW Washington, DC **2019**, p. CTu3A–4.
[131] Z. Ren, H. K.-H. So, E. Y. Lam, *IEEE Trans. Ind. Inform.* **2019**, *15*, 6179.
[132] T. Zeng, Y. Zhu, E. Y. Lam, *Opt. Express* **2021**, *29*, 40572.
[133] Y. Rivenson, Y. Zhang, H. Günaydn, D. Teng, A. Ozcan, *Light: Sci. Appl.* **2018**, *7*, 17141.
[134] M. L. Rivers, C. Gwinnett, L. C. Woodall, *Mar. Pollut. Bull.* **2019**, *139*, 100.
[135] Y. Zhu, Y. Li, J. Huang, E. Y. Lam, *Commun. Eng.* **2024**, *3*, 32.
[136] Y. Zhu, C. H. Yeung, E. Y. Lam, *J. Phys. Photonics* **2021**, *3*, 024013.
[137] H. Woo, K. Seo, Y. Choi, J. Kim, M. Tanaka, K. Lee, J. Choi, *Appl. Sci.* **2021**, *11*, 10640.
[138] S. Phan, C. K. Luscombe, *J. Appl. Phys.* **2023**, *133*, 020701.
[139] B. O. Asamoah, E. Uurasjärvi, J. Räty, A. Koistinen, M. Roussey, K.-E. Peiponen, *Polymers* **2021**, *13*, 730.
[140] J. Huang, W. Cai, Y. Wu, X. Wu, *Meas. Sci. Technol.* **2021**, *33*, 022001.
[141] T. Zeng, H. K.-H. So, E. Y. Lam, *Opt. Express* **2020**, *28*, 4876.
[142] L. Song, E. Y. Lam, in *Novel Techniques in Microscopy*, Optica Publishing Group, NW Washington, DC **2021**, pp. NTu1C–2.
[143] L. Song, E. Y. Lam, *Photonics Res.* **2022**, *10*, 758.
[144] K. W. Weiler, I. de Pater, *Astrophys. J. Suppl. Ser.* **1983**, *52*, 293.
[145] Thorlabs Inc., Pax5710m Polarization Camera, https://www.thorlabs.de/catalogpages/V21/1182.pdf (accessed: 2021).
[146] JAI Inc., Go-2400-pge Polarization Camera, https://www.jai.com/products/product-lines/go-series-single-sensor-area-scan-small-size (accessed: 2021).
[147] ASD Inc., ASD fieldspec Spectroradiometers, https://www.malvernpanalytical.com/en/products/product-range/asd-range/fieldspec-range (accessed: 2021).
[148] SPECIM Spectral Imaging Ltd., SPECIM IQ Hyperspectral Camera, https://andor.oxinst.com/products/ (accessed: 2021).
[149] C. A. Lindensmith, S. Rider, M. Bedrossian, J. K. Wallace, E. Serabyn, G. M. Showalter, J. W. Deming, J. L. Nadeau, *PloS One* **2016**, *11*, e0147700.
[150] S. Jericho, J. Garcia-Sucerquia, W. Xu, M. Jericho, H. Kreuzer, *Rev. Sci. Instrum.* **2006**, *77*, 043706.
[151] E. Serabyn, K. Liewer, C. Lindensmith, K. Wallace, J. Nadeau, *Opt. Express* **2016**, *24*, 28540.
[152] V. Dyomin, A. Davydova, S. Morgalev, N. Kirillov, A. Olshukov, I. Polovtsev, S. Davydov, *Front. Marine Sci.* **2020**, *7*, 653.
[153] Y. Li, Y. Zhu, J. Huang, Y.-W. Ho, J. K.-H. Fang, E. Y. Lam, *Sci. Rep.* **2024**, *14*, 2355.
[154] Y. Li, Y. Zhu, J. Huang, Y. Zhang, E. Y. Lam, in *Digital Holography and Three-Dimensional Imaging*, Optica Publishing Group, NW Washington, DC **2023**, p. HM1D–6.
[155] Y. Ye, K. Yu, Y. Zhao, *Sci. Total Environ.* **2022**, *818*, 151851.
[156] J. La Nasa, G. Biale, D. Fabbri, F. Modugno, *J. Anal. Appl. Pyrolysis* **2020**, *149*, 104841.
[157] A. M. Elert, R. Becker, E. Duemichen, P. Eisentraut, J. Falkenhagen, H. Sturm, U. Braun, *Environ. Pollut.* **2017**, *231*, 1256.
[158] S. Primpke, M. Godejohann, G. Gerdts, *Environ. Sci. Technol.* **2020**, *54*, 15893.
[159] C. F. Araujo, M. M. Nolasco, A. M. Ribeiro, P. J. Ribeiro-Claro, *Water Res.* **2018**, *142*, 426.
[160] J. Brandt, K. Mattsson, M. Hassellov, *Anal. Chem.* **2021**, *93*, 16360.
[161] L. Lv, X. Yan, L. Feng, S. Jiang, Z. Lu, H. Xie, S. Sun, J. Chen, C. Li, *Water Environ. Res.* **2021**, *93*, 5.
[162] M. N. Gerhard, D. Schymanski, I. Ebner, M. Esselen, T. Stahl, H.-U. Humpf, *Food Addit. Contam.: Part A* **2022**, *39*, 185.
[163] A. Tarafdar, S.-H. Choi, J.-H. Kwon, *J. Hazard. Mater.* **2022**, *432*, 128755.
[164] M. Jiao, S. Cao, L. Ren, R. Li, *J. Hazard. Mater. Adv.* **2021**, *3*, 100016.
[165] S. Harycki, A. Gundlach-Graham, *J. Anal. At. Spectrom* **2023**, *38*, 1.
[166] K. Bhagat, A. C. Barrios, K. Rajwade, A. Kumar, J. Oswald, O. Apul, F. Perreault, *Chemosphere* **2022**, *298*, 134238.
[167] Y. Hyeon, S. Kim, E. Ok, C. Park, *Chem. Eng. J.* **2023**, *454*, 140028.
[168] C. Tötzke, S. E. Oswald, A. Hilger, N. Kardjilov, *J. Soils Sediments* **2021**, *21*, 1476.
[169] H. Nelson, M. Woods, C. Lorenz, G. Gerdts, D. Fields, P. Matrai, M. Devoe, in *Ocean Sciences Meeting*, Oregon Convention Center Portland **2018**, p. 1.
[170] M. N. Woods, M. E. Stack, D. M. Fields, S. D. Shaw, P. A. Matrai, *Mar. Pollut. Bull.* **2018**, *137*, 638.
[171] P. Zheng, Q. Dai, Z. Li, Z. Ye, J. Xiong, H.-C. Liu, G. Zheng, S. Zhang, *Sci. Adv.* **2021**, *7*, eabg0363.
[172] S. Colburn, A. Zhan, A. Majumdar, *Sci. Adv.* **2018**, *4*, eaar2114.
[173] E. R. Fossum, in *Computational Optical Sensing and Imaging*, Optica Publishing Group, NW Washington, DC **2011**, p. JTuE1.
[174] G. Gallego, T. Delbrück, G. Orchard, C. Bartolozzi, B. Taba, A. Censi, S. Leutenegger, A. J. Davison, J. Conradt, K. Daniilidis, D. Scaramuzza, *IEEE Trans. Pattern Anal. Mach. Intell.* **2020**, *44*, 154.
[175] Z. Ge, Y. Gao, H. So, E. Y. Lam, *Opt. Lett.* **2021**, *46*, 3885.
[176] Z. Ge, P. Zhang, Y. Gao, H. K.-H. So, E. Y. Lam, *Opt. Express* **2022**, *30*, 2206.
[177] P. Zhang, Z. Ge, L. Song, E. Y. Lam, *IEEE Trans. Comput. Imag.* **2023**, *9*, 530.
[178] A. Spinelli, A. L. Lacaita, *IEEE Trans. Electron Devices* **1997**, *44*, 1931.
[179] F. Zappa, S. Tisa, A. Tosi, S. Cova, *Sens. Actuators A: Phys.* **2007**, *140*, 103.
[180] Y. Chi, A. Gnanasambandam, V. Koltun, S. H. Chan, in *16th European Conf. Computer Vision*, Springer, New York, NY **2020**, pp. 122–138.
[181] M. I. Jordan, T. M. Mitchell, *Science* **2015**, *349*, 255.
[182] L. Zhang, E. Y. Lam, J. Ke, *Opt. Express* **2022**, *30*, 3577.
[183] T. Zeng, E. Y. Lam, *IEEE Trans. Comput. Imag.* **2021**, *7*, 1080.
[184] Z. Ren, E. Y. Lam, J. Zhao, *IEEE Access* **2020**, *8*, 193512.
[185] X. Sun, N. H. Yung, E. Y. Lam, *IEEE Trans. Intell. Transp. Syst.* **2016**, *17*, 2594.
[186] J. Dong, L. Valzania, A. Maillard, T.-a. Pham, S. Gigan, M. Unser, *IEEE Signal Process. Mag.* **2023**, *40*, 45.
[187] H. Byeon, T. Go, S. J. Lee, *Opt. Laser Technol.* **2019**, *113*, 77.
[188] N. Meng, Z. Ge, T. Zeng, E. Y. Lam, *IEEE Access* **2020**, *8*, 116052.
[189] V. Evdokimova, S. Bibikov, A. Nikonorov, *Pattern Recognit. Image Anal.* **2022**, *32*, 466.
[190] M. Deng, S. Li, Z. Zhang, I. Kang, N. X. Fang, G. Barbastathis, *Opt. Express* **2020**, *28*, 24152.
[191] A. Lohia, K. D. Kadam, R. R. Joshi, A. M. Bongale, *Library Philosophy and Practice* **2021**, *4910*, 34.

[192] W. Ye, C. Liu, Y. Chen, Y. Liu, C. Liu, H. Zhou, *Signal Process. Image Commun.* **2023**, *110*, 116871.
[193] J. Chen, E. C. Frey, Y. He, W. P. Segars, Y. Li, Y. Du, *Med. Image Anal.* **2022**, *82*, 102615.
[194] Y. Luo, D. Mengu, N. T. Yardimci, Y. Rivenson, M. Veli, M. Jarrahi, A. Ozcan, *Light: Sci. Appl.* **2019**, *8*, 112.
[195] B. Shi, M. Patel, D. Yu, J. Yan, Z. Li, D. Petriw, T. Pruyn, K. Smyth, E. Passeport, R. D. Miller, J. Y. Howe, *Sci. Total Environ.* **2022**, *825*, 153903.
[196] W. Ai, G. Chen, X. Yue, J. Wang, *J. Hazard. Mater.* **2023**, *445*, 130568.
[197] J. Huang, Y. Zhu, Y. Li, E. Y. Lam, *ACS Photonics* **2023**, *10*, 4483.
[198] Y. Zhang, S. H. Chan, E. Y. Lam, *APL Photonics* **2023**, *8*, 5.
[199] F. Pizzurro, S. Recchi, E. Nerone, R. Salini, N. B. Barile, *Microplastics* **2022**, *1*, 303.
[200] N. Gao, Z. Huang, J. Xing, S. Zhang, J. Hou, *Front. Marine Sci.* **2021**, *8*, 762530.
[201] G. Van Horn, O. Mac Aodha, Y. Song, Y. Cui, C. Sun, A. Shepard, H. Adam, P. Perona, S. Belongie, in *Proc. of the IEEE Conf. on Computer Vision and Pattern Recognition*, IEEE, Piscataway, NJ **2018**, pp. 8769–8778.
[202] I. Jakubowicz, J. Enebro, N. Yarahmadi, *Polym. Test.* **2021**, *93*, 106953.
[203] C. Schwaferts, R. Niessner, M. Elsner, N. P. Ivleva, *Trends Anal. Chem.* **2019**, *112*, 52.

Yanmin Zhu received a B.S. in electrical and electronics engineering from KU Leuven, Belgium, in 2017, a B.Eng. from Southwest Jiaotong University, China, in 2017, an M.S. in optics and photonics from Imperial College London, UK, in 2018, and a Ph.D. from The University of Hong Kong, China, in 2023. She is currently a postdoctoral associate at the Massachusetts Institute of Technology, U.S. Her research interests include computational imaging, artificial intelligence, digital holography, and spectroscopy.

Yuxing Li received her B.S. in electronic science and technology from Shandong University in 2017 and her Ph.D. in precision medicine and healthcare from Tsinghua University in 2022. She was a visiting researcher at University of California, Berkeley, from 2018 to 2021. She is currently a postdoctoral fellow at the University of Hong Kong. Her research interests include computational imaging, digital holography, microplastics pollution assessment, and multimodal learning.

Jianqing Huang received his B.S. from Harbin Institute of Technology in 2017 and received his Ph.D. in power engineering from Shanghai Jiao Tong University in 2022. He was a visiting researcher at Lund University, Sweden, from 2019 to 2021. He is currently a postdoctoral fellow at the University of Hong Kong. His current research interests include computational optical imaging, combustion diagnostics and flow visualization, microplastics pollution assessment, and deep learning.

Yunping Zhang obtained a B.S. in electrical and electronic engineering from the University of Electronic Science and Technology of China, China, in 2018, and an M.S. in communications and signal processing from Imperial College London, UK, in 2019. Currently, she is pursuing her Ph.D. at the University of Hong Kong, China. Her research focuses on inverse imaging problems, digital holography, and physics-informed networks.

Yuen-Wa Ho received his B.Sc. in 2013 and his Ph.D. in cetacean ecology in 2021 from the School of Biological Sciences at the University of Hong Kong. He is currently a postdoctoral fellow at the Hong Kong Polytechnic University focusing on studies of microplastics. His research primarily explores cetacean ecology and the impact of microplastic pollution on the environment and marine organisms.

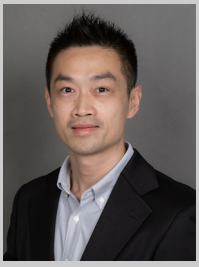

James Kar-Hei Fang obtained a B.Sc. from The University of Plymouth, UK, an M.Phil. from City University of Hong Kong, China, and a Ph.D. from The University of Queensland, Australia. He was a postdoctoral scientist at the Institute of Marine Research in Norway. Currently, he is an associate professor in the Department of Food Science and Nutrition at The Hong Kong Polytechnic University and principal investigator in State Key Laboratory of Marine Pollution at City University of Hong Kong. His research focuses on the analytical methodology of microplastics, their contamination in food, and their impacts on human health and ecosystems.

Edmund Y. Lam received his B.S., M.S., and Ph.D. in electrical engineering from Stanford University. He was a visiting associate professor with the Department of Electrical Engineering and Computer Science, Massachusetts Institute of Technology. He is currently a professor of electrical and electronic engineering at The University of Hong Kong. He also serves as the Computer Engineering Program Director and a research program coordinator with the AI Chip Center for Emerging Smart Systems. His research interest includes computational imaging algorithms, systems, and applications.